Mathematical Modelling of Truncated and Complete Denitrification and Dissimilatory Nitrate Reduction to Ammonium (DNRA) in Agricultural Soils

Tamara Kostyuk

A thesis submitted to the Faculty of Graduate studies in partial fulfillment of the requirements for the degree of Master of Science

Graduate Program in Applied and Industrial Mathematics

York University

Toronto, Ontario

©Tamara Kostyuk

August 2024

Abstract

Current agricultural fertilizers add nitrogen in the form of ammonium and nitrate to the soils where different bacteria enabled processes lead to formation of multiple nitrogen containing compounds included in the global nitrogen cycle. A better understanding of those processes can help control the anthropogenic contribution to greenhouse gases released from the soil as well as the nitrogen containing compounds accumulating in the soils and water sources. In our work, we analyse mathematical models of denitrifying and dissimilatory nitrate reduction to ammonium (DNRA) bacteria utilizing nitrogen oxides and organic carbon (acetate) as substrates. First, we consider a model implementing the Liebig's minimum principle for bacterial growth so that bacterial growth is limited by the most scarce substrate. We find this system's steady states and analyse its possible outcomes. Then we modify this model by including two Monod terms in the bacterial growth formulation, one for each substrate, to make the model more realistic and allow each substrate's concentration to influence the bacteria population's growth. We analyse this model's steady states and stability. We compare the two models and show how the changes in the model's structure affect the steady states feasibility and stability boundaries. We show how the system outcomes depend on the initial conditions (C/N ratio and concentrations) as well as the bacterial species' characteristics. Lastly, we explore truncated reactions with the addition of a third species.

Acknowledgements

I would like to say thank you to all people who have helped me to get through the challenging two years leading to this degree.

To my supervisor, Dr. Iain Moyles, thank you for your constant support and encouragement. I appreciate all your help and guidance for this project, as well as your advice on many other occasions over the last few years.

To my supervisory committee member, Dr. Woldegebriel Assefa Woldegerima, thank you for your feedback and valuable comments on this project that helped me to improve this thesis.

To my family, thank you for supporting me in many ways. In particular, to my husband Alex, there is no possible world in which I would be able to achieve any of my goals without you. I appreciate your endless love and your unwavering confidence in me.

Table of Contents

Abstract **ii**

Acknowledgments **iii**

Table of Contents **iv**

List of Tables **vi**

List of Figures **vii**

1 Chapter 1: Fate of nitrogen in soils **1**

1.1 Agricultural fertilizers and the nitrogen cycle 1

1.2 Denitrification and DNRA chemistry and biochemistry 3

1.2.1 Electron donors and acceptors 4

1.2.2 Bacteria performing denitrification and DNRA 5

1.3 Factors deciding the pathway (denitrification or DNRA) for nitrate in soil 6

1.4 Existing models and approach chosen for this project 7

1.5 Modelling principles for bacterium enabled processes 8

1.5.1 Liebig's minimum principle 10

1.5.2 Growth rate defined as a product of Monod terms 10

1.6 Summary 10

2 Chapter 2: Model for denitrification and DNRA competition with minimum principle for bacteria growth **12**

2.1 Model introduction 12

2.2 Steady state analysis 12

2.2.1 Steady states feasibility conditions 13

2.2.2 Steady states' stability analysis 19

2.3 Resource-ratio theory application to predict denitrifiers and DNRA bacteria competition outcomes 23

2.4 Summary 25

3 Chapter 3: Model for denitrification and DNRA competition with two terms bacterial growth definition **26**

3.1 Model justification and formulation 26

3.2 Non dimensional system and its analysis 26

3.2.1 Steady states 29

3.2.2 Stability analysis 35

3.2.3 Possibility and stability conditions for the coexistence steady state E3 38

3.3 A comparison between model with Liebeg's minimum principle and and model with two Monod terms in the growth rate definition 41

3.4 Summary 49

4 Chapter 4: Model for denitrification and DNRA competition with three bacterial species **51**

4.1 Model analysis 52

4.2 Numerical simulation and parameters choices 53

4.3 Model's sensitivity analysis 59

4.3.1 Latin Hypercube Sampling/Partial Rank Correlation Coefficient (LHS/PRCC) procedures 59

4.3.2 LHS/PRCC model analysis 60

4.4 Summary 63

5 Chapter 5: Conclusion and future work **64**

6 List of acronyms **66**

7 Bibliography **67**

List of Tables

1 Kinetic and stoichiometric parameters of denitrifiers and DNRA able bacteria used for model (9). 13

2 Comparison and possible combinations of feasibility and stability conditions for steady states "b only" E1 and "r only" E2. 38

3 Influent concentration, observed competition outcomes, measured biomass concentrations and substrates effluent concentrations at steady states in chemostat enrichment cultures reported in [48] - Case Study 1, and [49] - Case Study 2. 42

4 Simulation results for Case Study 1 for Model 1 (9) and Model 2 (12) 46

5 Simulation results for Case Study 2 for Model 1 and Model 2. 48

6 Parameter values used for simulations on 3 species model (41) 55

7 Simulations outcome for $\mu_{max,S} = 0.06\text{h}^{-1}$ 56

8 Simulations outcome for $\mu_{max,S} = 0.07\text{h}^{-1}$ 56

9 Simulations outcome for $\mu_{max,S} = 0.09\text{h}^{-1}$ 57

10 Simulations outcome for $\mu_{max,S} = 0.11\text{h}^{-1}$ 57

11 Parameter values range and baseline values for PRCC analysis 60

List of Figures

1 Schematic representation of the nitrogen cycle associated with soil fertilization. Volatilization (VLT), dissimilatory nitrate reduction to ammonia (DNRA), mineralization (MNL), assimilation (AS), immobilization (IM), nitrification (NF), atmospheric deposition (AD), denitrification (DNF) products. SOM stands for soil organic matter. Figure adapted from [31] 1

2 A schematic representation of the bacterial nitrogen cycles. 2

3 Growth rate defined by Monod function $\mu = \mu_{\max}\frac{S}{K_S+S}$. Values used are $\mu_{\max} = 0.5$ and $K_S = 10$. 9

4 Influent ratio k and nitrate influent concentrations required for "B only" steady states E1 and E2 establishment. 15

5 "B only" steady states: initial conditions (IC) leading to steady state with N=2 (E2) are shown in blue; initial conditions leading to steady state with C=10 (E1) are shown in aquamarine. . 15

6 Influent ratio k and the nitrate influent concentration correlation for R only steady states. . . 17

7 "R only" steady states: initial conditions leading to steady state with C=13/3 (E3) are shown in green; initial conditions leading to steady state with N=13/3 (E4) are shown in aquamarine 17

8 k and nitrate influent concentration correlation: for coexistence steady state to be established, k values should be between two curves. 18

9 R and B coexistence steady state. 19

10 Simulations outcome for IC with both bacterial population present with organic carbon influent concentration C_o fixed: for A, $C_o = 12$, for B, $C_o = 8$. 20

11 Simulations outcome for IC with both bacterial population present with nitrate influent concentration N_o fixed: for A $N_o = 3$, for B $N_o = 6$. 20

12 Simulations outcome for IC with only population B present (part A) and both population R and B present (part B). 21

13 Simulations outcome for IC with only population R present (part A) and both population R and B present (part B). 22

14 Possible outcomes of a system with two bacterial population. $N_o = 60$, C_o varies. 23

15 Graphical presentation of resource competition of two species (N1 and N2) competing for two resources (S and R). Blue lines represent minimal resource levels for species N2, and C2 is the consumption vector for species N2. Green line represent the minimal resource level for species N1, and C1 is the consumption vector for species N1. 24

16 Steady states for the non-dimentional system; blue curve shows "b only" state E1, green curve shows "r only" state E2, and the coexistence steady state E3 is shown with orange dot at two curves intersection. 35

17 Sample system trajectories with different influent ratio k for a E1b+E2a configuration. "r only" steady state E2a (possible trajectories shown in green) appears when n is a limiting substrate, and "b only" E1b (possible trajectories shown in blue) appears when c is a limiting substrate. Red lines show possible trajectories leading to coexistence steady state. 40

18 Sample dynamics for a system of configuration E1a+E2b with different initial k ratio. "r only" E2b (possible trajectories shown in green) appears when c is a limiting substrate, and "b only" E1a (possible trajectories shown in blue) appears when n is a limiting substrate. Yellow lines show possible trajectories leading to coexistence. 41

19 steady states found for model (9), referred to as Model 1, and model (12), referred to as Model 2. 43

20 Model (12) application to Case Study 1. Blue points show the initial condition of experiments resulting in DNRA domination, green point shows the initial condition of the experiment resulting in denitrifiers' domination, and orange points show the initial conditions leading to both species coexistence. 44

21 Model (9) application to Case Study 1. Blue points show the IC of experiments resulting in DNRA domination, green point shows the IC of the experiment resulting in denitrifiers' domination, and orange points show the IC leading to both species coexistence. 45

22 Models application to Case study 2. Graph A shows results for Model 1, and graph B shown results for Model 2. Blue points show the IC of experiments resulting in DNRA domincance, green point show the IC of the experiments resulting in denitrification dominance. 47

23 Simulations outcome for three species model. Parts A and B show results for $\mu_{\max,S} = 0.07$, parts C and D show results for $\mu_{\max,S} = 0.09$, parts E and F show results for $\mu_{\max,S} = 0.11$. Influent concentration of nitrate is 1000 μM. 58

24 PRCC results for the model with C/N influent ratio k=1.8 and k=2.2. In both cases model predicts outcome with three bacterial species coexistence. 62

1 Chapter 1: Fate of nitrogen in soils

1.1 Agricultural fertilizers and the nitrogen cycle

Nitrogen plays an important role in plants' development and growth impacting the yield and the quality of crops. The total nitrogen mass within the topsoil layer is between 0.1% to 0.6% of the soil weight, ranging from 2000 to 12000 kg$-$N ha^{-1}, depending on the type of soils [31]. Regular nitrogen fertilization aimed to replenish this nutrient availability every harvesting season has became a standard agricultural practice over the last century.

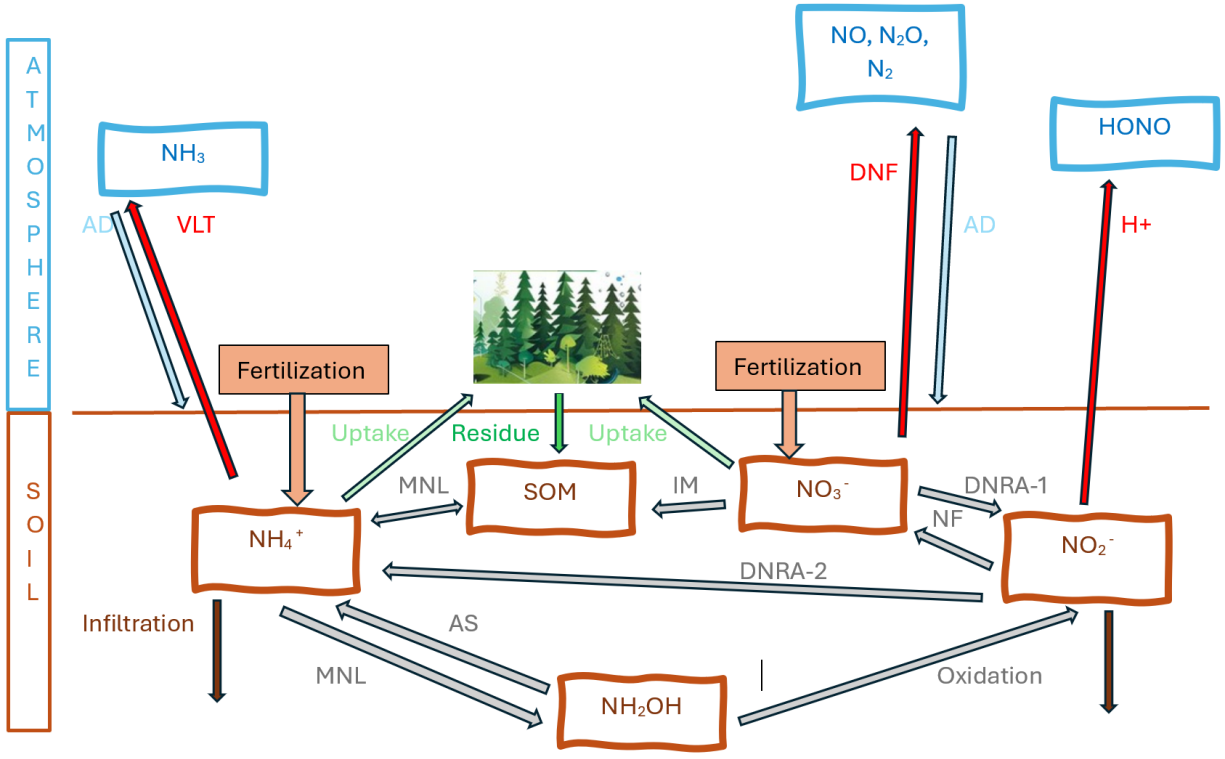


Figure 1: Schematic representation of the nitrogen cycle associated with soil fertilization. Volatilization (VLT), dissimilatory nitrate reduction to ammonia (DNRA), mineralization (MNL), assimilation (AS), immobilization (IM), nitrification (NF), atmospheric deposition (AD), denitrification (DNF) products. SOM stands for soil organic matter. Figure adapted from [31]

Current fertilizers used in agriculture contain nitrogen in the form of ammonia, nitrate, and other complex compounds (e.g urea, ammonium nitrate, etc.). When in the soil, there are various pathways for the nitrogen including direct uptake by plants, leaching to lower layers or ground water, and transformation via chemical and bacteria-enabled reactions (Figure 1). The chemical transformations involved in these

reactions are summarized in Figure 2. They are all redox reactions, and require, in addition to nitrogen containing species, that is oxidized (or reduced), a species serving an electron acceptor (or donor). Reactions oxidzing nitrogen, like nitrification and anaerobic ammonium oxidation (anammox), are shown with arrows going from left to right. Reactions reducing nitrogen, like denitrification and DNRA, are shown with arrows going from right to left. For those reactions reducing nitrogen, some organic carbon compounds, e.g. acetate ($C_2H_3O_2$) or formaldehyde (CH_2O) serve as an electron donor.

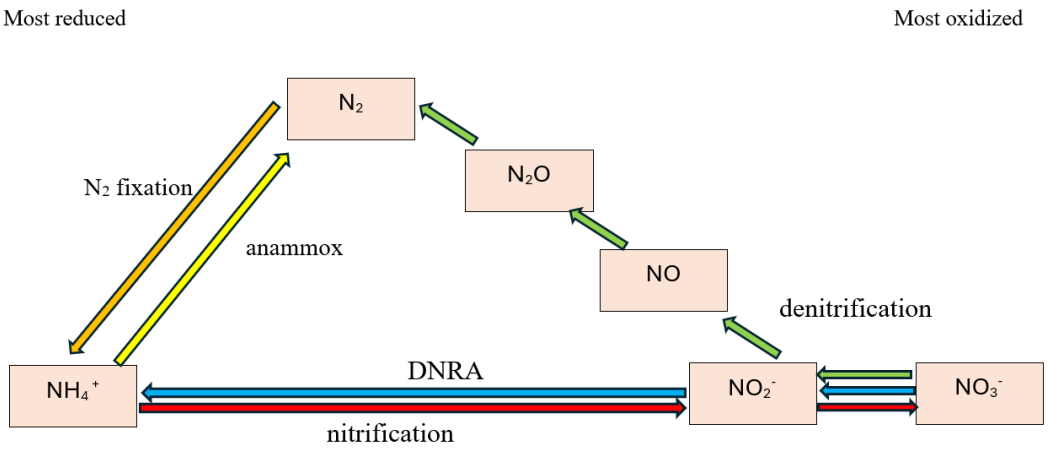


Figure 2: A schematic representation of the bacterial nitrogen cycles.

We will pay close attention to denitrification and DNRA that dominate nitrate reduction in anaerobic environments [44]. They both consist of microbial reduction of nitrate into a different nitrogen containing species. In denitrification, nitrate NO_3^- is reduced to nitrite NO_2^- and then to nitric oxide NO, nitrous oxide N_2O, and molecular nitrogen N_2. Denitrification functions as a sink for soil nitrate, since it converts nitrate to inert N_2 which is released to the atmosphere. However, other gaseous compounds that can be released during denitrification can be harmful for the environment - in particular, nitrous oxide N_2O is a potent greenhouse gas. Other intermediate products of denitrification, nitrite NO_2^- can form aqueous and gaseous HONO which, in turn, contributes to air pollution [53]. In Figure 1, those main nitrogen loss pathways are shown in red arrows.

DNRA (dissimilatory nitrate reduction to ammonium), consists of reducing nitrate to ammonium, and involves nitrate NO_3^- reduction to nitrite NO_2^-, and then to ammonium NH_4^+. Ammonium mostly stays in the soils and can be taken up by plants, however, under some conditions it is converted to ammonia NH_3 which volatilizes easily and contributes to air pollution by participating in haze formation [31]. Other

possible environmental risks are ammonium contamination due to its leaching to lower soil layers and air pollution by some amount of N_2O released in DNRA reaction as a by-product [33], [11], [23].

Excessive use of nitrogen fertilizers increases the soil nitrogen content, as well as the amount of nitrogen in the biosphere in general. Overall, anthropogenic factors doubled the level of nitrogen in the global cycle circulation [35]; in turn, as this added nitrogen goes through ecosystems, it is transformed into gaseous or organic soluble compounds that contribute to water and air pollution.

1.2 Denitrification and DNRA chemistry and biochemistry

Schluter et al. [36] notes the following basic requirements for denitrification in soil:

1. a shortage of O_2 as an electron acceptor;
2. the availability of $NO_3{}^-$ as an alternative electron acceptor;
3. the presence of a decomposable organic carbon compound supplying electrons for anaerobic respiration;
4. a microbial community that has the capacity to express the enzymes for some or all reduction steps in denitrification

DNRA generally happens in very similar physical conditions [33], with the main difference being in the nature of the microbial community that should be able to support the nitrate reduction to ammonium.

Complete denitrification involves four steps of nitrate reduction to molecular nitrogen N_2:

$$NO_3{}^- \rightarrow NO_2{}^- \rightarrow NO \rightarrow N_2O \rightarrow N_2 \tag{1}$$

In DNRA, the reduction goes as follows:

$$NO_3{}^- \rightarrow NO_2{}^- \rightarrow NH_4{}^+ \tag{2}$$

Chemical reactions involved in complete denitrification and DNRA are as follow (with formaldehyde CH_2O as a specific example of organic carbon) [16]:

$$\begin{aligned} &NO_3{}^- + \frac{1}{2}CH_2O \rightarrow NO_2{}^- + \frac{1}{2}HCO_3{}^- + \frac{1}{2}H^+ \\ &NO_2{}^- + \frac{3}{4}CH_2O + \frac{1}{2}H^+ \rightarrow N_2 + \frac{3}{4}HCO_3{}^- + \frac{1}{2}H_2O \\ &NO_2{}^- + H^+ + \frac{3}{2}CH_2O + \frac{1}{2}H_2O \rightarrow \frac{1}{2}CO_2 + HCO_3{}^- + NH_4{}^+ \end{aligned} \tag{3}$$

where the first two rows represent the overall complete denitrification; the first and the last rows represent DNRA.

Denitrification and DNRA activities are far from homogeneous in agricultural soils and can happen in what is called "hot spots" and "hot moments", where and when the conditions required for those reactions are met [13], [36].

1.2.1 Electron donors and acceptors

Bacteria need to gain energy for cellular activities and biomass growth. Many bacteria do it in a process called respiration. During respiration, a respiratory substrate (an organic carbon compound, the most common of them is glucose) is oxidized in the presence of an inorganic electron acceptor. Some of the substrate is utilized for biomass growth (and therefore is not completely oxidized), and some part is transformed into carbon dioxide:

$$\mathrm{a}(C_6H_{12}O_6) + \mathrm{b}(NH_3) + \mathrm{c}(O_2) \rightarrow \mathrm{d}(C_5H_7NO_2) + \mathrm{e}(CO_2) + \mathrm{f}(H_2O) \tag{4}$$

where $C_6H_{12}O_6$ is the substrate (in this case, glucose), $C_5H_7NO_2$ is the chemical formula for bacterial cell, ammonia NH_3 is the nitrogen source for the cell mass synthesis, and a, b, c, d, e, f are the stoichiometric coefficients [30]. The whole process is possible due to a bacteria mediated electron exchange between the carbon compound (as a donor) and the oxygen (as a terminal electron acceptor), with the energy released used by the bacteria for maintenance and the cell growth. This type of respiration, when oxygen is used as an electron acceptor, is called aerobic.

In anaerobic conditions, some bacteria are able to perform a similar process, with another chemical species becoming the terminal electron acceptor - anaerobic respiration. Some of those alternative electron acceptors are nitrate, manganese, iron, sulfate, and others.

Compound degradation in anaerobic conditions is often performed by a group of bacterial species each of which is performing a specialized reaction or reactions that together result in more or less complete substrate utilization [30].

Some bacterial species are able to perform aerobic respiration when oxygen is available, and switch to anaerobic respiration under low oxygen or anaerobic conditions - such bacteria are called facultative anaerobic.

Many bacteria species able to perform denitrification and DNRA are facultative anaerobic [44] and perform anaerobic respiration with nitrogen oxides used as a terminal electron acceptors. Hence, low oxygen or anaerobic conditions, as well as the availability of an nitorgen oxides species are necessary for denitrification

and DNRA.

The availability of an electron donor - an organic carbon source - is another necessary condition for both processes. Some carbon compounds, or substrates, are degraded easier and are utilized faster, some slower, which is reflected in the bacterial growth rate and the amount of energy obtained from any given substrate. Since there are many possible organic carbon compounds, to quantify the availability of electron donors, a measurement of oxygen required for a complete oxidation (to CO_2) of the given organic carbon compound is used - Chemical Oxygen Demand, or COD. COD is expressed SI units as milligrams per liter [$\mathrm{mg\,L^{-1}}$]. Then, the measured COD of a specific organic carbon compound can be used for computation in the redox reactions associated with denitrification and DNRA, even though O_2 is not directly involved in the process. Different carbon containing solutions have different COD and therefore can support different levels of efficiency of denitrification and DNRA [7], [33].

Denitrification and DNRA can also be performed with fermentable carbon sources, e. g. lactate, as the COD source for the reaction if a fermentative bacteria are included in the bacterial community. [50].

1.2.2 Bacteria performing denitrification and DNRA

The ability of a bacterium to perform denitrification or DNRA reactions is connected to the availability of genes encoding enzymes catalyzing the reduction of nitrate. Generally, enzymes make it possible for bacteria to transform the available compound into different compounds while deriving energy or molecules needed for biomass growth. Enzymatic reactions can generate large amount of energy that bacteria can use in their life cycle. There are normally many variations for each of the enzymes that are associated with different co-acting agents or environments. The enzymes necessary for denitrification are: nitrate reductase, nitrite reductase, nitric-oxide reductase, and nitrous-oxide reductase for the complete set of denitrification reactions [25]. Since nitrite reduction to NO is the first step that discriminates denitrification from DNRA, the ability to produce nitrite reductase enzyme is considered to be a definitive characteristic for denitrifying bacteria [38]. Bacteria lacking one or more of those enzymes will be only able to performs truncated denitrification, however, such bacteria occur quite frequently: Lycus et al. [25] show that out of 176 isolates from soil, altogether 70 isolates were able to perform at least one reduction step, including 30 species able to perform complete denitrification. Thus, truncated denitrification can substantially influence the overall denitrifying activities in soil [37], [25].

Bacteria performing DNRA are able to produce nitrate reductase for the first step of reducing NO_3^- to NO_2^- and a cytochrome c nitrite reductase to reduce NO_2^- to ammonium (without the release of any

intermediate) [23].

One of the classification of bacteria able to reduce NO_3^- is given in [33]:

1. denitrifiers, producing gaseous N compound;
2. NO_2^- accumulators which reduce NO_3^- only to NO_2^-;
3. DNRA microorganisms that reduce NO_3^- or NO_2^- to NH_4^+

Many studies investigating the abundance of microorganisms reducing NO_3^-, found that non-denitrifying bacteria outnumbers the denitrifiers: Gamble et al. [10] found the ratio of NO_2^- accumulator to denitrifiers to be about 4:1. More recent research suggest that there are much more denitrifying bacteria in soil [51],[25]; however, it is still believed that denitrifiers account for less than half of NO_3^- reducing community [21].

There are less studies of the distribution and diversity of DNRA capable bacteria, compared to denitrifying organisms. However, more recent research indicates that DNRA gives an important contribution to the nitrogen reducing in soils [39], [22], [47] which supports the idea that DNRA capable organisms should be more widely spread in different environments than it was believed before.

1.3 Factors deciding the pathway (denitrification or DNRA) for nitrate in soil

There are few factors deciding the pathway (denitrification or DNRA) that the nitrate will go. The most frequently referred to is the ratio COD/N$-NO_3$ [45], [33], [11], [3]. Organic carbon / nitrogen (in the form of COD/N$-NO_3^-$) ratio is generally a measure of the amount of electron donors per an electron acceptor. In low ratio conditions, when electron donors are limited and acceptors are in abundance, denitrification prevails, as it only requires 5 electrons per nitrate for the complete process. In high ratio conditions, with many electron donors available and less of acceptors present, DNRA prevails, with 8 electrons accepted by a nitrate. There are conditions, between "low" and "high", when both pathways happen concurrently. The specific values of the partitioning between denitrification and DNRA vary depending on the organic carbon source used as as a substrate [42], [7], [8]. Chakrawal et al. [3] show how the degree of reduction of the COD included in the system (and hence, the energy availability from the reduction) influences the bacterial growth rate and the partitioning between denitrification and DNRA.

Another important factor defining the fate of nitrate is the nutrients (organic carbon and nitrogen source) concentrations. It is shown experimentally that in a continuous (chemostat) culture with nutrients influent having the same COD/N$-NO_3$ ratio but different concentrations, different outcomes are possible [20] - from the complete extinction of one or both populations to their coexistence.

There are other factors that influence the partitioning between denitrification and DNRA and the overall efficiency for bacteria enabled processes in top soil - soil pH and physical characteristics (e.g. aggregate size and porosity), temperature, the dynamics of nutrients' influx, etc. [11], [33]. There is evidence that denitrification occurs more efficiently in planted soils and when plants are active (growing season), while DNRA predominates in unplanted soils or when plant activity is low [33]. Overall, the regulation mechanisms governing the competition between denitrification and DNRA in soils are not yet fully described and are the object of interest for further study.

1.4 Existing models and approach chosen for this project

The nitrogen cycle and the fate of nitrogen in agricultural soils has attracted scientific interest for many years, first mostly in the context of agricultural productivity, and later also in the context of greenhouse gases (primarily N_2O and CO_2) released to the atmosphere [9].

Heinen [17] gives the following classification for denitrification sub-models in N cycling models (which can be extended to models of any bacteria-enable processes in soils): 1) microbial growth models that explicitly include the dynamics of microorganisms responsible for N cycling processes; 2) soil structural models that consider physical characteristics of the top soil (aggregate size, porosity) with N-cycling processes based on diffusion of gases and the aggregates distribution, and 3) simplified processes models that do not include microbial dynamics or gaseous diffusion, but rather determine the denitrification rate from easier measurable parameters, such as degree of soil saturation with water, soil temperature and nitrate content of the soil.

Del Grosso et al. [5] also divide modelling methods used to quantify nitrogen budget in three groups, but this division is based on the spatial scale and temporal resolution. 1) models with emission factors based on global data sets. Such models normally assume uniformity in soil properties, weather, vegetation cover, landscape management, and have large spatial and temporal scale (e.g. estimate global annual greenhouse gases emission). 2) Models with emission factors based on regional data sets. These models consider soil properties as a moderate level (plot scales from m^2 to ha) and have temporal resolution of a day or less. Usually they do not explicitly represent the microbial dynamics, but can account for microbial impact implicitly. 3) Models including 3-D soil structure and properties, such as pore size and aggregates distribution. Those models have high spatial ($\sim$ mm) and temporal (hours or less) resolution and usually include processes - such as microbial activity and O_2 flow.

The classifications given by Heinen and Del Grosso agree in so far as the scale and the level of details expected from a model's predictions dictate the type of the model and corresponding methods. Del Grosso et

al. point out that explicit representation of microbial dynamics has potential to improve model performance but it comes with the cost of increased complexity and increased uncertainties in model outputs because microbial related model parameters are usually not well constrained.

We use a model that includes explicit bacterial dynamics necessary for investigation of two populations' competition and potential coexistence, and chemical species involved into both denitrification and DNRA reactions and the final products of denitrification (N_2) and DNRA ($NH_4{}^+$). We will assume uniformity in soils characteristics and will not include any spacial dynamics for the bacteria to keep the model as simple as possible. However, taking into account the bacteria population dynamics should add accuracy to the model output.

1.5 Modelling principles for bacterium enabled processes

One of the widely used approach to model ecological systems involving bacterial growth is based on Monod equation [30]:

$$\mu = \mu_{\max} \frac{S}{K_S + S} \tag{5}$$

where μ is the specific growth rate for the bacterium species ([time^{-1}]), $\mu_{\max}$ is the maximum specific growth ([time^{-1}]), S is the concentration of the substrate S, ([mass $\cdot$ volume^{-1}]), and K_S is the half-saturation constant, or affinity constant for the given substrate ([mass $\cdot$ volume^{-1}]) . Both $\mu_{\max}$ and K_S are found experimentally. $\mu_{\max}$ is the maximum possible growth of the given organism under optimal conditions, and K_S is defined as the substrate concentration at which growth occurs at one half the value of $\mu_{\max}$ (Figure 3).

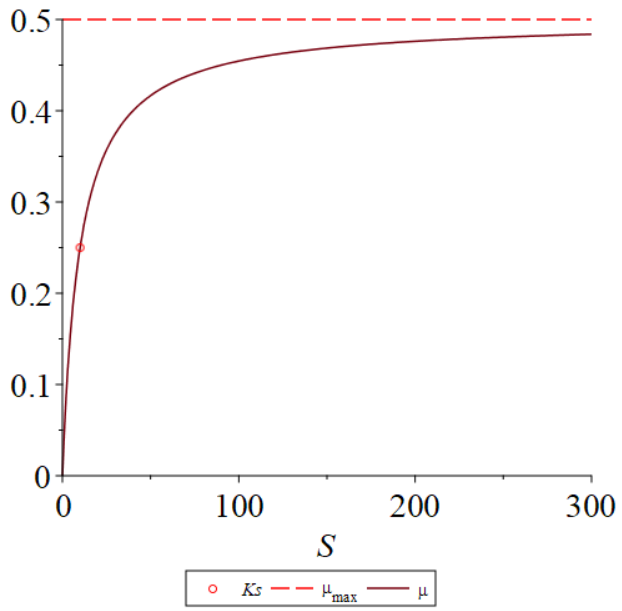


Figure 3: Growth rate defined by Monod function $\mu = \mu_{\max} \frac{S}{K_S+S}$. Values used are $\mu_{\max} = 0.5$ and $K_S = 10$.

The limiting cases for Monod equation are if $S >> K_S$, then $\mu \approx \mu_{\max}$, and if $S << K_S$, then $\mu \approx \mu_{\max} \frac{S}{K_S}$, a linear function of the substrate concentration.

Another important parameter is yield which represents the measurement of the substrate utilization by the bacterium for the biomass generation. It is defined as the unit amount of cell mass produced per unit amount of substrate consumed/degraded, ($[\text{mass} \cdot \text{mass}^{-1}]$). The more efficiently the substrate is utilized, the higher the value of the yield coefficient is. Then, the substrate usage (degradation) can be expressed in terms of microbial growth:

$$\frac{dS}{dt} = -\frac{1}{Y_{XS}} \frac{\mu_{\max,X} S}{K_S + S} X \tag{6}$$

where S is the concentration of the substrate S, Y_{XS} is the yield of bacterium X on substrate S, $\mu_{\max,X}$ is the maximum specific growth of$X$, and K_S is the affinity constant for X and S, and X is the given bacterium population size ($[\text{mass} \cdot \text{volume}^{-1}]$).

A complete model would consist of differential equations describing changes in chemical and biological species included in the system. In most models found in the literature, denitrification and DNRA reactions are considered as one step, so bacteria performing denitrification supports all reduction reactions from NO_3^- through N_2 production, and DNRA capable bacteria supports reduction from NO_3^- to NH_4^+. We first build and analyse model following this approach, and then investigate the model of truncated and complete

denitrification and DNRA with two steps reactions and three bacterial species included.

1.5.1 Liebig's minimum principle

Liebig's law of the minimum states that the growth rate of a species is dictated not by total resources available, but by the most limited resource out of all resources necessary. This law is applied to biological and ecological models of bacterial growth that include multiple nutrients / substrates. The growth rate of a bacterium species based on two nutrients availability is defined as

$$\min\left(\mu_{\max 1}\frac{S_1}{S_1+K_{S1}}, \mu_{\max 2}\frac{S_2}{S_2+K_{S2}}\right) \tag{7}$$

where $\mu_{\max i}$ is the maximum bacterium growth rate for the given substrate, S_1 and S_2 are the concentrations of the available substrates, and K_{Si} is the corresponding affinity constant.

The benefit of this approach is its simplicity, however, such a system will be harder to analyze by mathematical methods due to a non-differentiable function involved. Another, even more important consideration is that connecting the growth rate to one most limiting substrate only is not always desirable as it cuts off the real life complex system too severely thus preventing the model to reflect a deeper cooperation of multiple environmental factors to shape the processes in question [43].

1.5.2 Growth rate defined as a product of Monod terms

A different approach is to define a bacterium's growth rate as the product of a few separate Monod terms, one for each substrate available so that the concentration of each resource impacts the resulting growth rate.

$$\mu = \mu_{\max}\left(\frac{S_1}{S_1+K_{S1}}\right)\left(\frac{S_2}{S_2+K_{S2}}\right)\left(\frac{S_3}{S_3+K_{S3}}\right) \tag{8}$$

This approach is used in many models, for example for water treatment processes that might include multiple factors (nutrients) for bacteria growth [14], and to model soil bacteria growth [24], [29]. Models implementing this approach might be more computationally demanding, but they are also more realistic as bacterial growth in nature is defined by a complex of environmental factors.

1.6 Summary

In Chapter 1, we explained the connection between common fertilization practices in agriculture and their possible influence to the global nitrogen cycle and increased release of greenhouse gases. We discussed the

role of denitrification and DNRA reactions in the nitrogen cycle as well as the environmental conditions necessary for both. Also, we described different approaches to modelling bacteria enables processes and outlined the approach we use.

2 Chapter 2: Model for denitrification and DNRA competition with minimum principle for bacteria growth

2.1 Model introduction

The first model consists of four ODE - for two substrates and two for bacterial species:

$$\begin{aligned}
\frac{dN}{dt} &= (N_o - N)D - \frac{1}{Y_{BN}}\mu_B(C,N)B - \frac{1}{Y_{RN}}\mu_R(C,N)R \\
\frac{dC}{dt} &= (C_o - C)D - \frac{1}{Y_{BC}}\mu_B(C,N)B - \frac{1}{Y_{RC}}\mu_R(S,R)R \\
\frac{dB}{dt} &= [\mu_B(C,N) - D]B \\
\frac{dR}{dt} &= [\mu_R(C,N) - D]R
\end{aligned} \tag{9}$$

where B is the concentration of DNRA able bacteria, R is the concentration of denitrifiers, and N and C are the concentrations of nitrate and organic carbon correspondingly, N_o and $C_o = kN_o$ are influent concentrations (with influent concentrations ratio $\frac{C_o}{N_o} = k$), D is dilution rate, and Y_{XZ} is the yield of species X per unit of resource Z consumed (mole biomass per mole substrate).

$\mu_X(C,N)$ denotes the growth rate of species X on two substrates - nitrate and organic carbon, and is defined as follows:

$$\mu_X(C,N) = \min\left(\mu_{\max,X}\frac{C}{K_{XC}+C}, \mu_{\max,X}\frac{N}{K_{XN}+N}\right) \tag{10}$$

where $\mu_{\max,X}$ is the maximum growth rate of species X ($[\mathrm{h}^{-1}]$), K_{XC} and K_{XN} are half-saturation constant of species X for substrate C or N correspondingly. All concentrations values and affinity constants are expressed in [μM].

In the next few sections we perform mathematical analysis of this model.

2.2 Steady state analysis

Parameter values that we used for computation, simulations, and analysis of the model formulated in (9) are given in Table 1 [48]:

Table 1: Kinetic and stoichiometric parameters of denitrifiers and DNRA able bacteria used for model (9).

parameter	meaning	value	units
$\mu_{\max,R}$	maximum growth rate for R	0.086	h^{-1}
Y_{RN}	yield for unit of biomass of R per unit nitrate consumed	0.431	1
Y_{RC}	yield for unit of biomass of R per unit COD consumed	0.488	1
K_{RN}	affinity constant for R to nitrate	10	μM
K_{RC}	affinity constant for R to COD	10	μM
$\mu_{\max,B}$	maximum growth rate for B	0.052	h^{-1}
Y_{BN}	yield for unit of biomass of B per unit nitrate consumed	0.656	1
Y_{BC}	yield for unit of biomass of B per unit COD consumed	0.488	1
K_{BN}	affinity constant for B to nitrate	2	μM
K_{BC}	affinity constant for B to COD	10	μM

There are six steady states for the system (9): one for both species extinct, two for B only surviving, two for only R surviving, and one coexistence steady state. First, we will show the steady states feasibility condition, and then we will look into their stability.

2.2.1 Steady states feasibility conditions

The steady states for the system are as follow:

1. E0: $\{B = 0, C = C, N = N, R = 0\}$, both species are extinct; in this case $N = N_o$ and $C = C_o = kN_o$, there k represents the C_o/N_o, the ratio of the influent concentrations.

2. E1: $\{B = B, C = 10, N \geq 2, R = 0\}$. This steady state is feasible for $N_o > 2$ and C_o/N_o ratio $\frac{10}{N_o} < k < \frac{1.344 \cdot 10^{-8}(1.000 \cdot 10^{8} N_o + 5.439 \cdot 10^{8})}{N_o}$.
   For the smallest influent concentration, when $N_o \to 2$, $k \to 5$, however, when $N_o \to \infty$ the ratio $0 < k < 1.344$.

   There are two alternative solutions for N and B for this steady state:

   (a) E1a

$$\begin{aligned} B &= 0.488kN_o - 4.880 \\ N &= -0.744kN_o + 7.439 + N_o \end{aligned}.$$

(b) E1b

$$B = \frac{0.244(61.k^2N_o^2 - 82.kN_o^2 - 1384.kN_o + 820.N_o + 7740.)}{(61.kN_o - 82.N_o - 610.)}$$

$$N = -0.744kN_o + 7.439 + N_o$$

3. E2: $\{B = B, C > 10, N = 2, R = 0\}$. This steady state is feasible for $N_o > 2$ and C_o/N_o ratio $k > \frac{5.000 \cdot 10^{-9}(2.688 \cdot 10^8 N_o + 1.462 \cdot 10^9)}{N_o}$ so that the maximum $k \to 5$ is when $N_o \to 2$, and $k \to 1.344$ when $N_o \to \infty$. This steady state also has two alternative solutions for B and C:

   (a) E2a

$$B = 0.656N_o - 1.312$$

$$C = kN_o - 1.344N_o + 2.689$$

   (b) E2b

$$B = \frac{0.328(61.kN_o^2 - 82.N_\circ^2 - 122.kN_o + 938.N_o - 1548.)}{(61.kN_o - 82.N_o + 164.)}$$

$$C = kN_o - 1.344N_o + 2.688$$

The relationship between the influent ratio k and the nitrate concentration required for E1 and E2 states is shown on figure 4: E2 is established when k value is above the curve, and E1 is established when k value is below it.

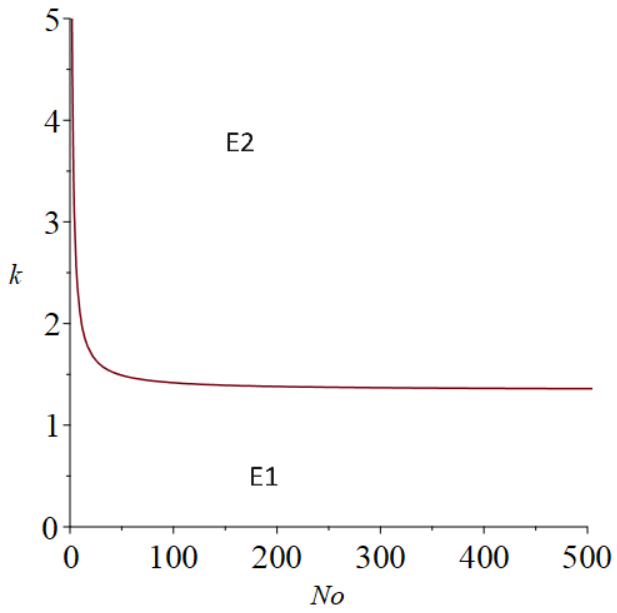


Figure 4: Influent ratio k and nitrate influent concentrations required for "B only" steady states E1 and E2 establishment.

Figure 5 shows the initial conditions (the N_o/C_o grid), leading to each steady state:

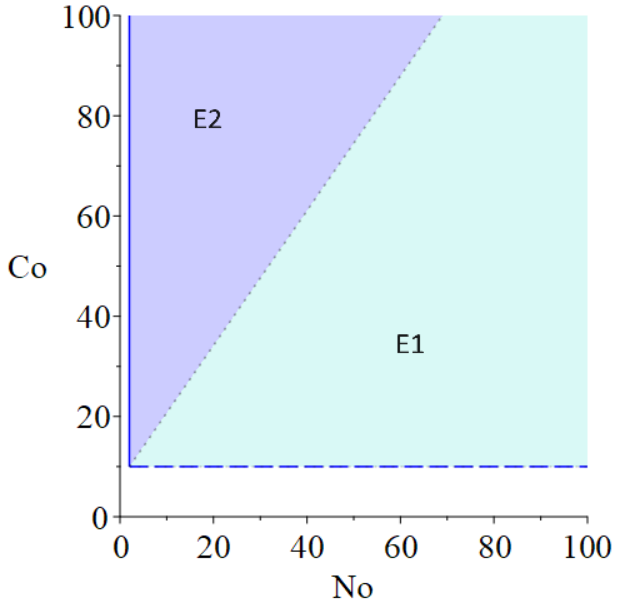


Figure 5: "B only" steady states: initial conditions (IC) leading to steady state with N=2 (E2) are shown in blue; initial conditions leading to steady state with C=10 (E1) are shown in aquamarine.

4. E3: $\{B = 0, C = \frac{13}{3}, N \geq \frac{13}{3}, R = R\}$, feasible for $N_o > 13/3$ and
$\frac{4.333}{N_o} < k < \frac{8.832 \cdot 10^{-10}(5.731 \cdot 10^8 + 1.000 \cdot 10^9 N_o)}{N_o}$,
with $k \to 1$ as $N_\circ \to 13/3$, and $0 < k < 0.883$ as $N_o \to \infty$. Two alternative solutions for N and R are as follows:

   (a) E3a

$$R = 0.488kN_\circ - 2.115$$

$$N = N_\circ - 1.132kN_\circ + 4.906$$

   (b) E3b

$$R = \frac{5.674 \cdot 10^{-10}(3.137 \cdot 10^{25}k^2N_\circ^2 - 2.770 \cdot 10^{25}kN_\circ^2 - 5.489 \cdot 10^{26}kN_\circ + 1.201 \cdot 10^{26}N_\circ + 1.790 \cdot 10^{27})}{1.206 \cdot 10^{17}kN_\circ - 1.066 \cdot 10^{17}N_\circ - 5.228 \cdot 10^{17}}$$

$$N = N_\circ - 1.132kN_\circ + 4.906$$

5. E4: $\{B = 0, C > \frac{13}{3}, N = \frac{13}{3}, R = R\}$, which is feasible for $N_o > \frac{13}{3}$ and
$k > \frac{1.000 \cdot 10^{-10}(8.832 \cdot 10^9 N_o + 5.061 \cdot 10^9)}{N_o}$
with $k \to 1$ as $N_o \to 13/3$, and $k \to 0.883$ as $N_o \to \infty$. Two alternative solutions for C and R for E4 are below:

   (a) E4a

$$R = 0.431N_\circ - 1.868$$

$$C = kN_\circ - 0.883N_\circ + 3.827$$

   (b) E4b

$$R = \frac{5.012 \cdot 10^{-10}(1.508 \cdot 10^{24}kN_\circ^2 - 1.332 \cdot 10^{24}N_\circ^2 - 6.535 \cdot 10^{24}kN_\circ + 2.662 \cdot 10^{25}N_\circ - 9.036 \cdot 10^{25})}{(5.800 \cdot 10^{15}kN_\circ - 5.123 \cdot 10^{15}N_\circ + 2.220 \cdot 10^{16})}$$

$$C = kN_\circ - 0.883N_\circ + 3.827$$

The correlation between required k and the nitrate influent concentration for the establishment of R only steady state is shown on figure 6. For E3, k is expected to be below the curve, for E4, k should be above the curve.

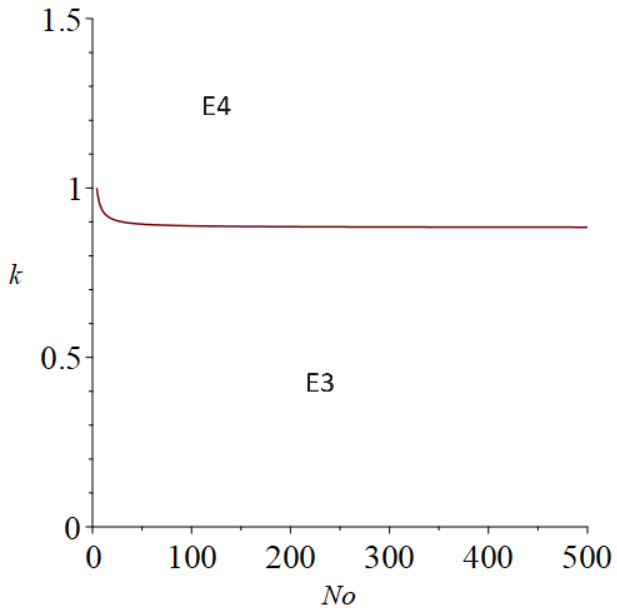


Figure 6: Influent ratio k and the nitrate influent concentration correlation for R only steady states.

Both R only steady states are shown on N_o/C_o grid on figure 7.

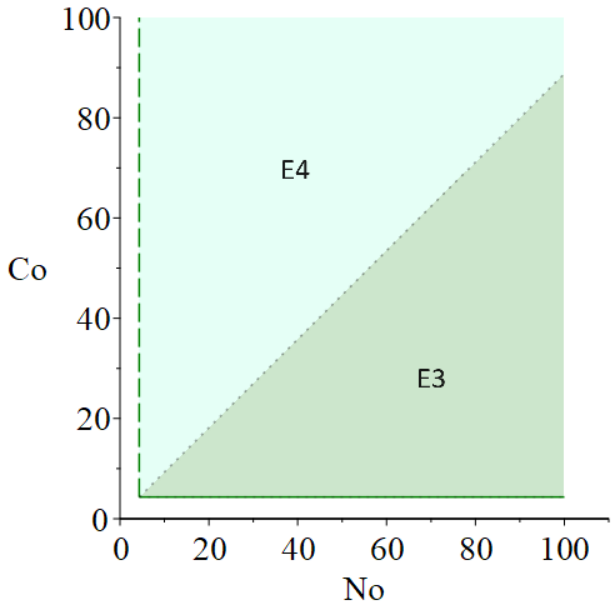


Figure 7: "R only" steady states: initial conditions leading to steady state with C=13/3 (E3) are shown in green; initial conditions leading to steady state with N=13/3 (E4) are shown in aquamarine

6. E5: $\{C = 10., N = \frac{13}{3}, B > 0, R > 0\}$ coexistence steady state. It is feasible for $N_o > 13/3$ and substrates influent ratio within the following values:
$$\frac{2.109 \cdot 10^{-9}}{(4.189 \cdot 10^{8} N_o + 2.928 \cdot 10^{9})} N_o < k < \frac{1.070 \cdot 10^{-9}}{(1.257 \cdot 10^{9} N_o + 3.903 \cdot 10^{9})} N_o$$
For smaller influents concentrations, larger C_o/N_o ratio is required: as $N_o \to 13/3$, $k \to 2.308$, while with $N_o \to \infty$ substrates influent ratio is $0.883 < k < 1.344$. Correlation between k and nitrate influent concentration for coexistence steady state to be established is shown on figure 8.

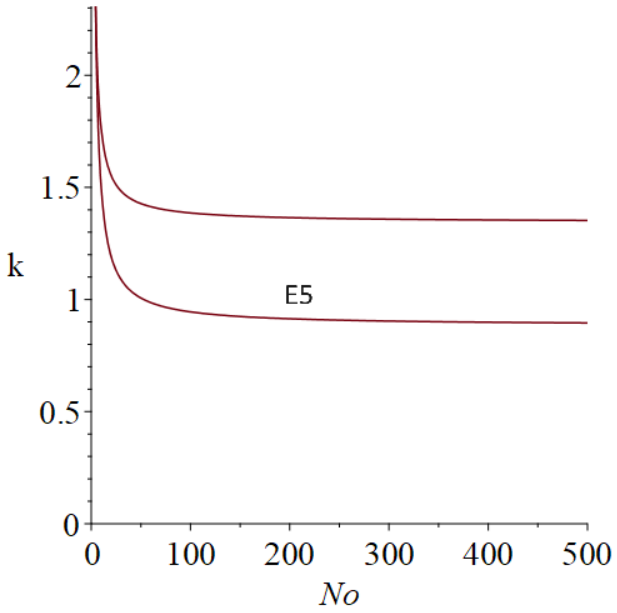


Figure 8: k and nitrate influent concentration correlation: for coexistence steady state to be established, k values should be between two curves.

Solutions for R and B are as follows:

$$B = 1.423kN_o - 1.257N_o - 8.783$$

$$R = -0.935kN_o + 1.257N_o + 3.903$$

The initial conditions leading to coexistence steady state are shown on figure 9 on N_o/C_o grid.

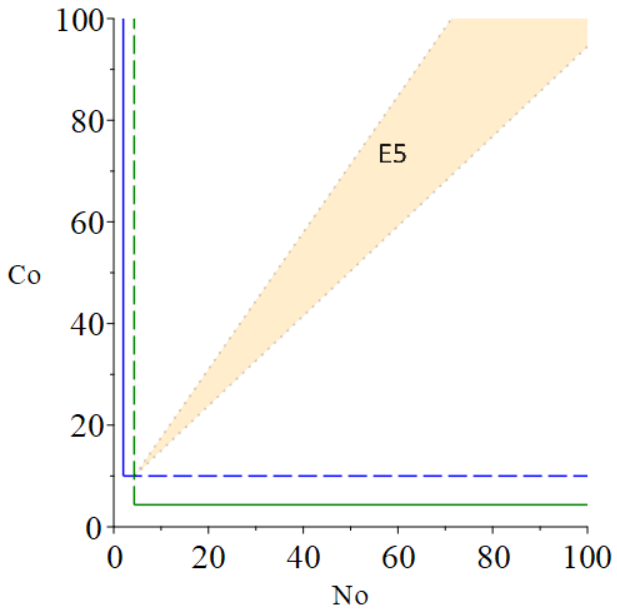


Figure 9: R and B coexistence steady state.

2.2.2 Steady states' stability analysis

We now investigate if these steady states are stable with regard to perturbations, and what are the conditions for their stability. However, stability analysis by standard methods for the system (9) is complicated due to a non-smooth min function used in the model. Instead, we will use simulations and try to draw conclusion based on the simulations outcome.

The outcomes of the simulations only have solutions "a" for E1, E2, E3, and E4, so all the conclusions we draw for the corresponding states stability are about steady states E1a, E2a, E3a, and E4a. Since solutions "b" never appear in the simulation we consider the corresponding states E1b, E2b, E3b, and E4b not stable.

1. E0 (degenerate steady state). To check the condition for its stability we ran simulations with both bacterial populations present, and influent concentrations changing from below the minimum required for both species survival to above those values. Figure 10 shows the simulations results for nitrate influent concentration varying from 0.5 μM to 14.5 μM and organic carbon influent fixed at 12μM or 8 μM.

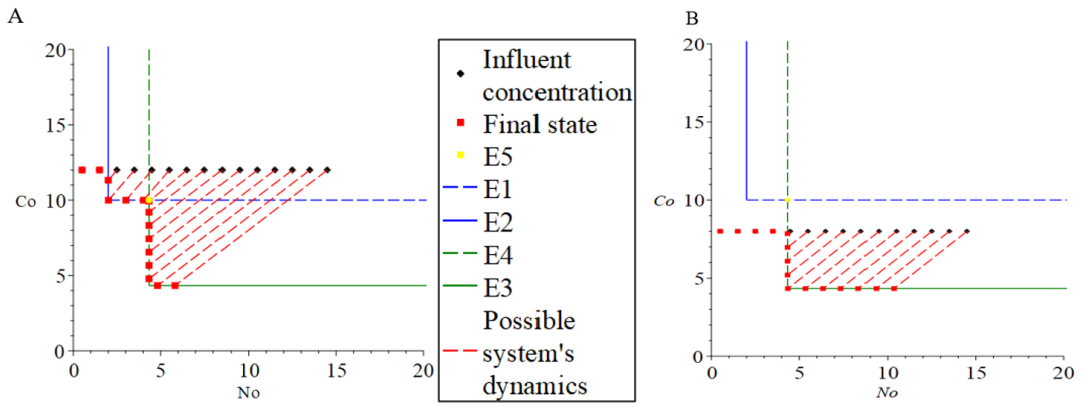


Figure 10: Simulations outcome for IC with both bacterial population present with organic carbon influent concentration C_o fixed: for A, $C_o = 12$, for B, $C_o = 8$.

In Figure 10 part A we can see that E0 is stable for nitrate influent $N_o < 2$, or below the feasibility requirements for E2. Once $N_o \geq 2$, any steady state is possible, depending on the influent ratio. Similarly, in part B we can see that at a lower level of carbon influent concentrations, E0 is stable when $N_o < 13/3$, or the feasiblilty condition for E4. Once $N_o \geq 13/3$, E3 or E4 is possible, depending on the influent concentrations.

If N_o is fixed, and C_o varies from 2 to 16, we can see that E0 is only stable when C_o level is below the feasibility requirements for E1 and E3 (see Figure 10).

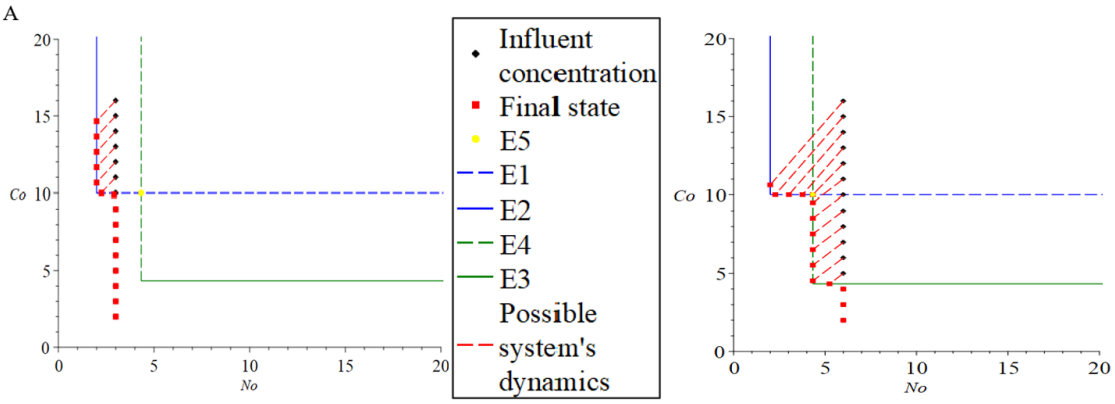


Figure 11: Simulations outcome for IC with both bacterial population present with nitrate influent concentration N_o fixed: for A $N_o = 3$, for B $N_o = 6$.

In Figure 11 part A, E0 is only stable when $C_o < 10$, the minimum feasibility condition for E1; once $C_o \geq 10$, both E1 and E2 are possible, depending on the influent ratio. In part B, E0 is stable when $C_o < 13/3$, the mininmum feasibility condition for E3, and once $C_o \geq 13/3$, all steady state are possible, depending on the influent concentrations.

Based on the simulation results we can conclude that E0 is stable when $\{N_o < 2$ or $C_o < 13/3$ or $(N_o < 13/3$ and $C_o < 10)\}$.

2. To check the stability for "B only" state E1 and E2, we will compare simulations' outcomes with various influent ratios and IC including only population B or both bacterial populations.

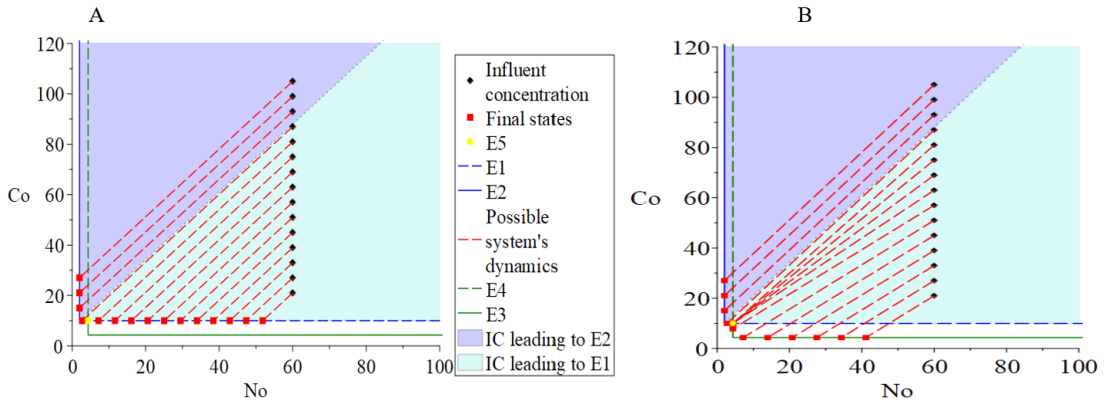


Figure 12: Simulations outcome for IC with only population B present (part A) and both population R and B present (part B).

As it can be seen, E2 is stable for both types of systems - with only population B present and both populations R and B present. However, E1 is only stable in one species systems and becomes unstable once a second population is introduced.

3. To check the stability for "R only" state E3 and E4, we will use the same strategy as in the previous case.

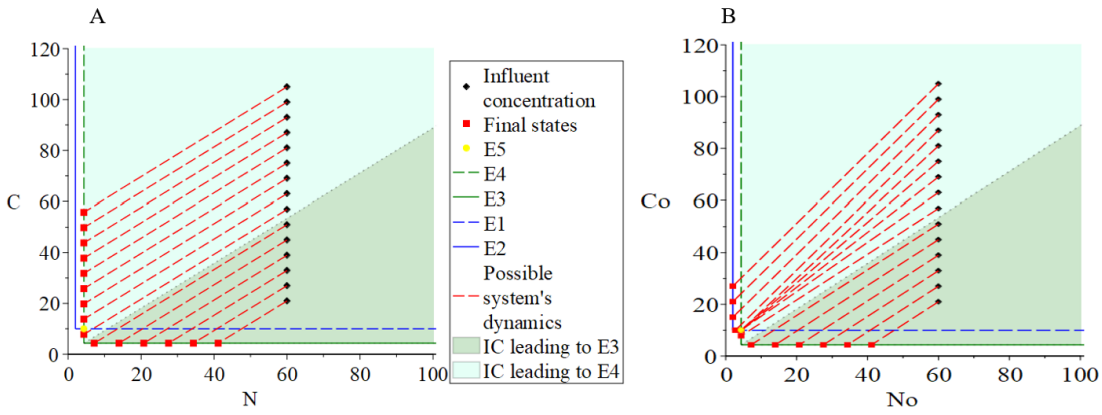


Figure 13: Simulations outcome for IC with only population R present (part A) and both population R and B present (part B).

From comparing part A and part B in figure 13, we can conclude that E4 is only stable for a truly one species systems, however, if another bacteria is introduced, only E3 is stable.

4. As we can see in Figures 12 and 13, E5 coexistence steady state appears to be stable for a range of IC areas laying between zones leading to "R only" and "B only" steady states.

We can conclude that for a two species system (with non-zero initial condition for both bacterial populations), with influent concentration exceeding the minimal feasibility requirements for non-degenerate steady states, there are five possible outcomes resulting from the actual ratio of the nitrate and acetate influent concentrations. "B only" E1 and "R only" E4 appear for a very limited C_o to N_o ratios, while three other steady states - E2, E3, and E5 cover most of the outcomes space (Figure 14).

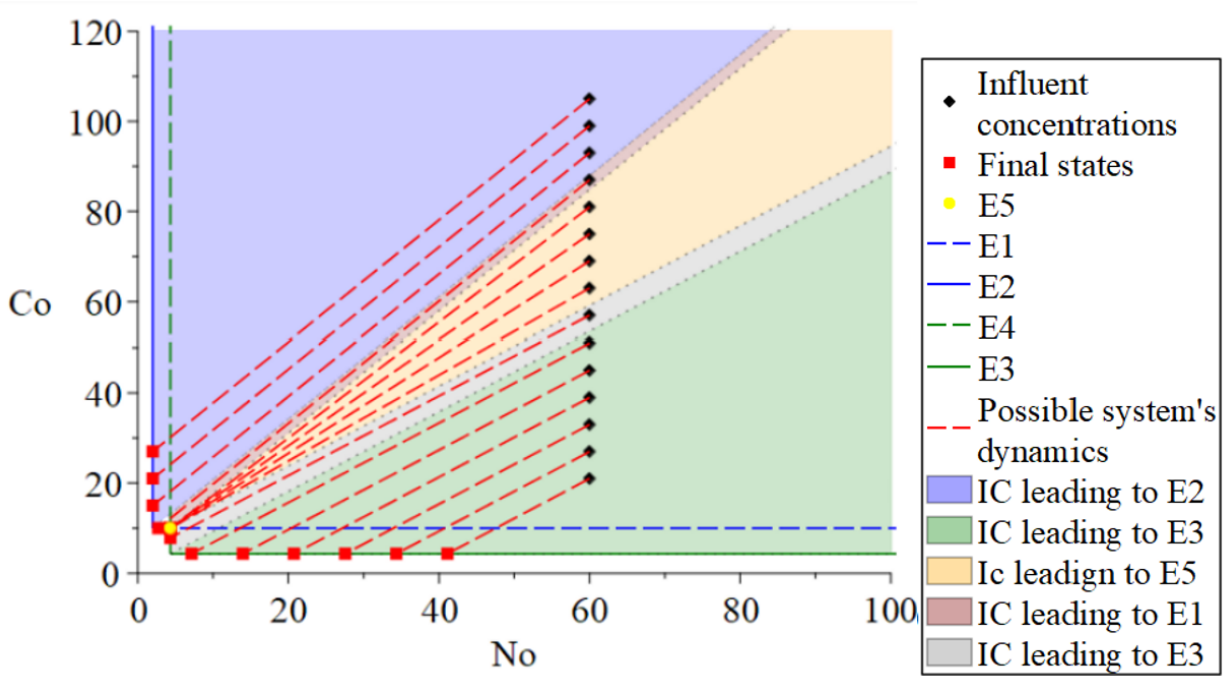


Figure 14: Possible outcomes of a system with two bacterial population. $N_o = 60$, C_o varies.

2.3 Resource-ratio theory application to predict denitrifiers and DNRA bacteria competition outcomes

It is interesting to see what other ways were used to predict denitrifiers and DNRA able bacteria competition outcome in a system with two substrates. Jia et al. [20] performed analysis using the resource-ratio theory to predict the outcome of two species competitions and check their model on experimental data. We will give a quick review of the resource-ratio theory and then will see how their results relate to our findings.

Resource-ratio theory was first proposed by Robert MacArthur in 1972 [26], and then extended and developed by David Tilman [46]. The resource-ratio theory assumes that there is a dynamic relationship between the resources and consumers. If two species consume the same resource than the species able to grow at the lower resource level, J_R, will prevail in the competition. When two species are competing for two different limiting resources, resource-ratio theory predicts that either one species can dominate by having a lower J_R's for both resources, or a trade-off can appear if each species has lower J_R for a different resource. In this last case species dominance is decided by the ratio on the resources available, and both species may be able to coexist at intermediate ratios of the resources supply. However, trade-offs of J_R does not guarantee the coexistence, its possibility depends on resource supply and each species' resource

consumption rate. The most general criteria for the possibility of two species coexistence is if supply rate and a species' consumption rate restricts its own growth more than it restricts the growth of the other species - then coexistence is possible.

A general picture of possible outcomes is shown on Figure 15:

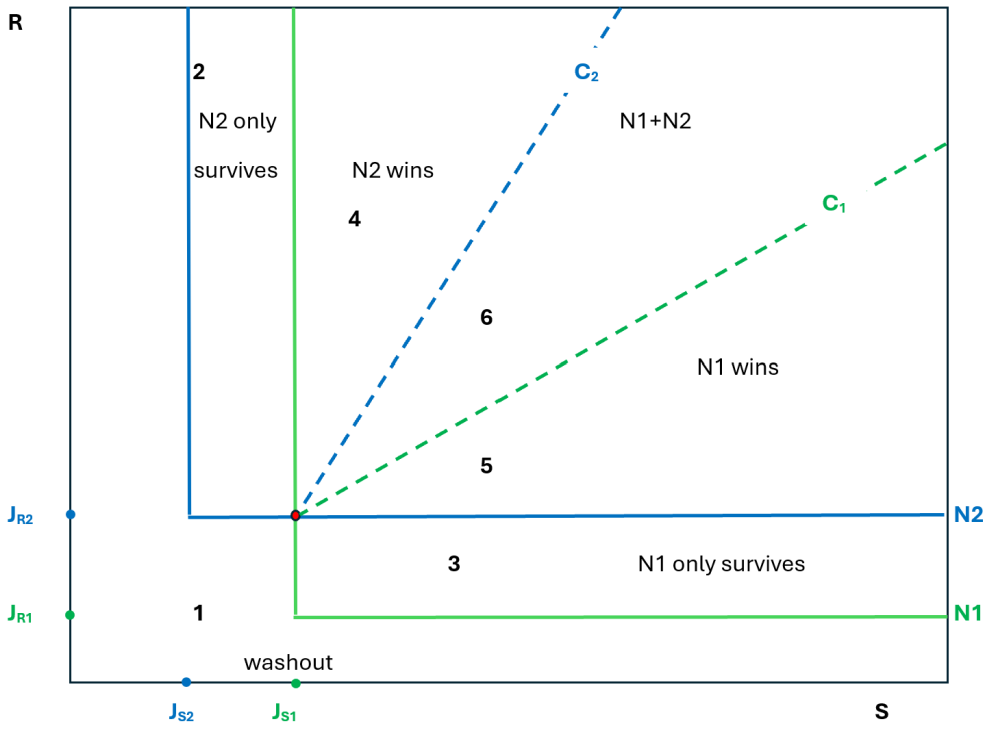


Figure 15: Graphical presentation of resource competition of two species (N1 and N2) competing for two resources (S and R). Blue lines represent minimal resource levels for species N2, and C2 is the consumption vector for species N2. Green line represent the minimal resource level for species N1, and C1 is the consumption vector for species N1.

Solid lines N1 and N2 corresponds to minimal resource concentrations and mark the limits of each species survival, C_1 and C_2 are consumption vectors for the corresponding species. In region 1, both species are extinct, in region 2 only species N2 survive, in region 3 only species N1 survives. The competition outcome in regions 4, 5 and 6, depends on the position of the supply points (influent concentrations) and is governed by the consumption vector. In zone 4, N2 wins the competition and eventually pushes N1 to extinction; in zone 5, N1 eventually outcompetes N2, and both species can stably coexist in region 6.

Resource-ratio theory has been applied to various models in ecology, see for example [6], [19], [28].

Jia et al. [20] used resource-ratio theory to describe interactions between two microbial species - denitrifiers and DNRA able bacteria and used model (9) for numerical computation of the predicted values using parameter values shown in Table 1.

Predicted outcomes found by Jia et al. (see Figure 2 in [20]) align well with the result of the mathematical analysis of the steady state of model (9). However, mathematical analysis of the system's steady states provides us with more insights about the nature of the model's observed steady states and their dependence on the system's parameters.

2.4 Summary

In Chapter 2, we introduced a model for denitrifiers and DNRA able bacteria competing over nitrate and organic carbon substrate with Liebig's minimum principle included into the bacterial growth rate definition. We found the systems' steady states and analysed their feasibility. Then, we ran simulations to observe the stability conditions for each steady states and found five possible systems' steady states and outlined the conditions for each of them to emerge.

3 Chapter 3: Model for denitrification and DNRA competition with two terms bacterial growth definition

3.1 Model justification and formulation

One of the drawbacks of the model (9) is the difficulty of performing its stability analysis using standard methods due to a non-differentiable function in the bacterial growth rate formulation. Even more importantly, when a bacterium uses two (or more) substrates, there is no reason to think that only the most limiting one defines the bacterium growth. The availability of other substrates almost surely influences the population growth. Accordingly, it would make the model more realistic if the growth rate includes components reflecting each substrate's availability. In the new model we change the bacterial growth rate definition:

$$\mu_X = \mu_{X,\max} \frac{N}{K_{XN} + N} \frac{C}{K_{XC} + C} \tag{11}$$

to now include two Monod terms, one for each substrate, so that each substrate's availability contributes to the bacterium growth.

The process modelling ODE equations are not changed but bacterial growth rate μ_X is now defined as in (11):

$$\begin{aligned}
\frac{dB}{dt} &= (\mu_B - D)B \\
\frac{dR}{dt} &= (\mu_R - D)R \\
\frac{dN}{dt} &= (N_o - N)D - \frac{1}{Y_{BN}}\mu_B B - \frac{1}{Y_{RN}}\mu_R R \\
\frac{dC}{dt} &= (C_o - C)D - \frac{1}{Y_{BC}}\mu_B B - \frac{1}{Y_{RC}}\mu_R R
\end{aligned} \tag{12}$$

In the next section, we perform a detailed mathematical analysis of the system.

3.2 Non dimensional system and its analysis

Due to the system's complexity, we will non-dimensionalize the model (12) and then perform its analysis.

Let $N = \bar{N}n$, $C = \bar{C}c$, $B = \bar{B}b$, $R = \bar{R}r$ and $t = \bar{t}\hat{t}$, where $\bar{X}$ is dimensional, and x and $\hat{t}$ are

dimensionless. The non-dimensional models becomes:

$$\begin{aligned}
\dot{n} &= \bar{t}D\left[\left(\frac{N_0}{\bar{N}} - n\right)D - \frac{\mu_{B,max}\hat{\mu_B}\bar{B}b}{DY_{BN}\bar{N}} - \frac{\mu_{R,max}\hat{\mu_R}\bar{R}r}{DY_{RN}\bar{N}}\right] \\
\dot{c} &= \bar{t}D\left[\left(\frac{C_0}{\bar{C}} - c\right)D - \frac{\mu_{B,max}\hat{\mu_B}\bar{B}b}{DY_{BC}\bar{C}} - \frac{\mu_{R,max}\hat{\mu_R}\bar{R}r}{DY_{RC}\bar{C}}\right] \\
\dot{b} &= \bar{t}D\left[\left(\frac{\mu_{B,max}\hat{\mu_B}}{D} - 1\right)b\right] \\
\dot{r} &= \bar{t}D\left[\left(\frac{\mu_{R,max}\hat{\mu_R}}{D} - 1\right)r\right]
\end{aligned} \tag{13}$$

where

$$\hat{\mu_X} = \frac{n}{k_{xn} + n}\frac{c}{k_{xc} + c} \tag{14}$$

Each non-dimensional affinity constant $k_{xy} = \frac{K_{XY}}{Y_o}$ is scaled by the corresponding substrate's influent concentration, so its value can be relatively large, if influent concentration is small compared to K_{XY}, or small, if influent concentrations is much larger than the corresponding K_{XY}.

We can scale time with the dilution rate by letting $\bar{t} = D^{-1}$, so that the time step in the system is defined by how fast (or slowly) influents run into and out of the system. Also, we will scale N and C with influent concentrations by letting $\bar{N} = N_o$ and $\bar{C} = C_o$. We can scale bacteria with carbon sink term: $\bar{B} = \dfrac{DY_{BC}C_o}{\mu_{B,max}}$ and $\bar{R} = \dfrac{DY_{RC}C_o}{\mu_{R,max}}$. Then, we will define the following parameters:

$$\begin{aligned}
\beta &= \frac{\mu_{B,max}}{D} \\
\nu &= \frac{\mu_{R,max}}{\mu_{B,max}} \\
G &= \frac{C_o Y_{BC}}{N_o Y_{BN}} \\
Y &= \frac{Y_{RC}Y_{BN}}{Y_{RN}Y_{BC}}
\end{aligned} \tag{15}$$

Parameters groupings β and $\beta\nu$ show how the maximum growth rate of each bacterial species correlates with the dilution rate. Evidently, we would expect this ratio to be larger that 1 in order for a bacterium to survive in a system with the given dilution rate D, otherwise the bacteria is washed out.

Parameters G and GY include ratios of the influent concentrations C_o/N_o and the yield ratio of each bacterial species on the corresponding substrate. These parameter groupings show how efficiently each bacteria produces biomass on the consumed substrates and shows each substrate's relative contribution to the bacterium growth. If G or GY larger than 1, that would mean that organic carbon influent contributes more to the corresponding bacterium's growth. If those parameters are smaller than 1, nitrate influent would

have a larger impact on the bacterium growth. Then, the dimensionless system becomes:

$$\begin{aligned}
\dot{n} &= 1 - n - \hat{\mu_B} Gb - \hat{\mu_R} GYr \\
\dot{c} &= 1 - c - \hat{\mu_B} b - \hat{\mu_R} r \\
\dot{b} &= (\beta \hat{\mu_B} - 1)b \\
\dot{r} &= (\beta \nu \hat{\mu_R} - 1)r
\end{aligned} \tag{16}$$

with $n(0) = 0, c(0) = 0, b(0) = \delta_b, r(0) = \delta_r$ and $\delta_x = \dfrac{X(0)}{\bar{X}}$. δ_r and δ_b parameters represent the corresponding bacteria biomass concentration "surviving" the dilution of the system and thus constitutes the initial bacteria population.

There are some important assumptions that we need to make about the system. As it was mentioned before, affinity constants k_{xy} can be relatively small, $k_{xy} << 1$, and then the bacteria growth rate

$$\hat{\mu_X} = \frac{n}{k_{xn} + n} \frac{c}{k_{xc} + c} \approx 1 \tag{17}$$

Such approximation correspond to saturation case, when substrate influent are much larger thatn the corresponding affinity constant, and bacterium growth approaches its maximum. The opposite case is when $k_{xy} >> 1$ so that

$$\hat{\mu_X} << 1 \tag{18}$$

which corresponds to bacteria starvation scenario with an influent concentrations are comparable to or smaller than the corresponding affinity constants.

For this model, we will assume that the system is at saturation. The main reason for this is that it is generally acknowledged that agricultural fertilizers are used in excessive quantities, and a lot of nitrogen is not immediately used by the plant and can stay in the soil for longer time. According to the information provided by the *Agriculture and Agri-Food Canada*, the residual soil nitrogen, mostly in the form in nitrate, in 2016 amounted to 21 kg per ha [2]. Assuming that the nitrogen is located in the top 20 cm of arable lands, this amount translates into about 750μM.

The assumption of the system being in saturation is also true for the chemostat experiments data on denitrifiers and DNRA able bacteria competition that was reported in literature (see for example [49], [48], [50]).

Now, using the fact that all k_{xy} are small, we can relate them to each other which should be useful later

on in the analysis:

$$\begin{aligned} k_{bn} &= \epsilon \\ k_{bc} &= a_1\epsilon \\ k_{rn} &= a_2\epsilon \\ k_{rc} &= a_3\epsilon \end{aligned} \tag{19}$$

where $\epsilon << 1$ and $a_i = O(1)$.

In the next section, we will analyse the steady states of the system.

3.2.1 Steady states

Similar to the approach in Chapter 2, we will first introduce the steady state and talk about their feasibility, and then look into stability conditions. There are four steady states in the system:

1. E0 - degenerate steady state with with $r = 0, b = 0, n = 1, c = 1$.
2. E1 - "b only" steady state, with population r extinct: $\{b = b, c = \dfrac{a_1\epsilon(n+\epsilon)}{n(\beta-1)-\epsilon}, n = n, r = 0\}$.

   The complexity of the system did not allow to find the solutions for this steady state directly so we used perturbation methods to find the approximate solution.

   First, the value of n is found to be the solution to the quadratic:

$$(\beta-1)n^2 + (-Ga_1\epsilon + G\beta - G - \beta - \epsilon + 1)n - a_1\epsilon^2 G - \epsilon G + \epsilon) \tag{20}$$

   Then, we will find an approximate solution for n, and will use it to find the corresponding values for b and c. To approximate n we assume $n = n_0 + n_1\epsilon + n_2\epsilon^2$ where $\epsilon << 1$ - that assumption was explained in Section 3.2 in more detail. More terms can be included into expression for n if higher accuracy is needed.

   On the next step, we use the expression for n in the equation 20:

$$(\beta-1)(n_0 + n_1\epsilon + n_2\epsilon^2)^2 + (-Ga_1\epsilon + G\beta - G - \beta - \epsilon + 1)(n_0 + n_1\epsilon + n_2\epsilon^2) - a_1\epsilon^2 G - \epsilon G + \epsilon \tag{21}$$

expand it and collect terms of O(1), O(ϵ) and O(ϵ^2):

$$\begin{aligned} &O(1) : G\beta n_0 + \beta n_0^2 - Gn_0 - \beta n_0 - n_0^2 + n_0 \\ &O(\epsilon) : (-Ga_1 n_0 + G\beta n_1 + 2\beta n_0 n_1 - G\epsilon n_1 - \beta\epsilon n_1 - 2\epsilon n_0 n_1 - G - n_0 + n_1 + 1)\epsilon \\ &O(\epsilon^2) : -Ga_1 n_1 + G\beta n_2 + 2\beta n_0 n_2 + \beta n_1^2 - Ga_1 - Gn_2 - \beta n_2 - 2n_0 n_2 - n_1^2 - n_1 + n_2 \end{aligned} \tag{22}$$

Solving for n_0, n_1, and n_2 and if necessary, for more terms, allows to approximate the value of n to the desired accuracy. We are using answer of accuracy O(ϵ) so we are only interested in n_0 and n_1.

Two roots for n_0 are

$$n_{01} = 0, n_{02} = -G + 1 \tag{23}$$

Two corresponding roots for n_1 are

$$n_{11} = \frac{1}{\beta - 1}, n_{12} = \frac{Ga_1}{\beta - 1} \tag{24}$$

Then, we have two solutions for n:

(a) solution a): $n = 0 + \frac{1}{\beta - 1}\epsilon$;

(b) solution b): $n = -G + 1 + \frac{Ga_1}{(\beta - 1)}\epsilon$

Using those values for n, we can find the other solutions. We found two sets of solutions for E1, both to the accuracy of O(ϵ):

(a) solution E1a:

$$\begin{aligned} n &= \frac{\epsilon}{\beta - 1} \\ c &= \frac{G - 1}{G} + \frac{a_1\epsilon}{\beta - 1} \\ b &= \frac{\beta}{G} - \frac{\beta\epsilon}{G(\beta - 1)} \\ r &= 0 \end{aligned} \tag{25}$$

The feasibility condition (when all values are positive) are as follows: from $n > 0$ we need $\beta > 1$, and from $c > 0$ and $b > 0$ we have $G > \frac{\beta - 1}{\beta - 1 + a_1\epsilon}$ and $\beta > 1 + \epsilon$. Combining those condition, we can conclude that E1a is feasible when

i. $\beta > 1 + \epsilon$

ii. $G > \dfrac{\beta - 1}{\beta - 1 + a_1\epsilon}$

(b) solution E1b follows from the second value of n shown before

$$\begin{aligned} n &= (1 - G) + \frac{G a_1 \epsilon}{\beta - 1} \\ c &= \frac{a_1 \epsilon}{\beta - 1} \\ b &= \beta - \frac{\beta a_1 \epsilon}{(\beta - 1)} \\ r &= 0 \end{aligned} \tag{26}$$

This set of solutions is feasible if

i. $\beta > 1 + a_1\epsilon$

ii. $0 < G < \frac{\beta - 1}{\beta - 1 - a_1\epsilon}$

Comparing the solution, we can see that in each pair one of the values depends on parameter G (and hence, on the influent concentrations ratio) and the other does not: in E1a n is independent of G, while c and b depend on it. In E1b, n value depends on G, and c and b do not. The possible reason is that each solution reflects the system outcome under one of the substrate's limitation. If a resource is abundant and exceeds the species' maximum consumption ability, its final amount in the system will be reflective of the supply level and the bacteria consumption, so in terms of our system, the final amount would depend on G or GY. If, however, a resource is strictly limited, its final amount in the system will only show the quantity corresponding the minimum limit of species's ability to consume, no dependence on G or GY. Accordingly, E1a can be an equilibirum that is formed under n limiting conditions, and E1b can be an steady state formed under c limiting condition. We will check this hypothesis later on and will see if there are any implications regarding the system performance.

3. E2 - "r only" steady state with population b extinct: $\{b = 0, r = r, n = n, c = \dfrac{a_3\epsilon(a_2\epsilon + n)}{\beta\nu(n-1) - a_2\epsilon}\}$. We use perturbation methods to find the solution, similar to E1. There are two sets of solution, both of accuracy $O(\epsilon)$:

(a) E2a:

$$\begin{aligned} n &= \frac{a_2\epsilon}{\beta\nu - 1} \\ c &= \frac{GY - 1}{GY} + \frac{a_3\epsilon}{\beta\nu - 1} \\ r &= \frac{\beta\nu}{GY} - \frac{\beta\nu a_2\epsilon}{(\beta\nu - 1)GY} \\ b &= 0 \end{aligned} \tag{27}$$

steady state E2a is feasible if

i. $\beta\nu > 1 + a_2\epsilon$.

ii. $GY > \dfrac{\beta\nu - 1}{\beta\nu - 1 + a_3\epsilon}$

(b) E2b

$$\begin{aligned} n &= (1 - GY) + \frac{GY a_3\epsilon}{\beta\nu - 1} \\ c &= \frac{a_3\epsilon}{\beta\nu - 1} \\ r &= \beta\nu - \frac{\beta\nu a_3\epsilon}{(\beta\nu - 1)} \\ b &= 0 \end{aligned} \tag{28}$$

This set of solutions is feasible if

i. $\beta\nu > 1 + a_3\epsilon$.

ii. $0 < GY < \dfrac{\beta\nu - 1}{\beta\nu - 1 - a_3\epsilon}$

Just like in E1 solutions, in E2a n does not depend on GY which contains information about influent ratio, and c and r depend on it, and in E2b the dependence is reversed. Based on the reasoning presented earleir, we would expect E2a to describe an steady state formed under n limitation, and E2b an steady state formed under c limitation.

4. E3 - coexistence steady state, with two sets of solutions.

(a) solution E3a

$$
\begin{aligned}
n =& \frac{((-\beta\nu + d + 1)a + a_3(\beta-1)d + \sqrt{W} - a_3)\epsilon}{2a_1\beta\nu - 2\beta a_3 - 2a_1 + 2a_3} \\
c =& \frac{\epsilon a_1((\beta\nu + a_2 - 1)a_1 + ((\beta-1)a_2 - 2\beta + 1)a_3 + \sqrt{W})}{((\beta-1)a_2 - (\beta+1)(\beta\nu-1))a_1 + (\beta-1)(a_3(\beta-1)a_2 + \sqrt{W} + a_3)} \\
b =& \frac{\beta(P+\sqrt{W})}{Q}\left(-\frac{(2\beta\nu-2)(\beta\nu+a_2-1)(GY-1)a_1^2}{2}\right. \\
& + (((\nu(GY-1)\beta^2 + (-GY+1)\nu\beta)a_2 + (GY-1)\beta(\beta\nu-1))a_3 + (\beta\nu-1)\sqrt{W}(GY-1))a_1 \\
& - ((1+(\beta-1)a_2)a_3 + \sqrt{W})a_3(\beta-1)(GY-1)) \\
& - \epsilon(2\beta\nu-2)(GY(a_2-1)a_3 - \frac{\beta\nu+a_2-1}{2})a_1^2 \\
& + (2GY(\beta-1)(a_2-1)a_3^2 + ((\beta-1)a_3^2 + (-2\beta^2\nu+2)a_2 + \beta\nu - 1)a_3 - (\beta\nu-1)\sqrt{W})a_1 \\
& \left. +((1+(\beta-1)a_2)a_3 + \sqrt{W})a_3(\beta-1)a_2)\right) \\
r =& \frac{\nu\beta(\sqrt{W}+V)}{T}\left(\left(-\frac{(-\beta\nu+1)a_1 + a_3(\beta-1)a_2)}{2}\sqrt{W} + (G(a_2-1)a_3 - \frac{\nu\beta+a_2-1}{2}(\beta\nu-1)a_1^2\right.\right. \\
& - a_1a_3(G(\beta-1)(a_2-1)a_3 - \nu a_2\beta^2 + \frac{a_2^2+\nu}{2}\beta - \frac{(a_2-1)^2}{2}) \\
& \left.-\frac{a_3^2(\beta-1)(\beta a_2 - a_2 + 1)a_2}{2}\right)\epsilon \\
& + \frac{(\beta-1)(G-1)a_3 - (\beta\nu-1)(G-1)a_1}{2}\sqrt{W} + \frac{(\beta\nu+a_2-1)(G-1)(\beta\nu-1)a_1^2}{2} \\
& -a_1a_3\left(\frac{\nu((G-1)a_2+G-1)\beta^2}{2} - \frac{\nu(G-1)a_2+G-1}{2}\beta\right) + \frac{a_3^2(\beta-1)(\beta a_2-a_2+1)(G-1)}{2}\Bigg)
\end{aligned}
\tag{29}
$$

where

$$
\begin{aligned}
W &= (a_1\nu - a_2a_3)^2\beta^2 + 2(a_2-1)(a_1-a_3)(a_1\nu + a_2a_3)\beta + (a_2-1)^2(a_1-a_3)^2 \\
P &= (\beta\nu + a_2 - 1)a_1 + (-1 + (-\beta+1)a_2)a_3 \\
Q &= (4a(a_2-1)G((a_1\nu - a_3)\beta - a_1 + a_3)((a_2-\nu)\beta - a_2 + 1)(Y-1)a_3) \\
T &= 2((\beta\nu-1)a_1 - a_3(\beta-1))a_3(a_2-1)((a_2-\nu)\beta - a_2 + 1)Ga_1(Y-1) \\
V &= (\beta\nu + a_2 - 1)a_1 - a_3(\beta a_2 - a_2 + 1)
\end{aligned}
$$

(b) solution E3b

$$
\begin{aligned}
n =& \frac{((-\beta\nu + d + 1)a + a_3(\beta-1)d - \sqrt{W} - a_3)\epsilon}{2a_1\beta\nu - 2\beta a_3 - 2a_1 + 2a_3} \\
c =& \frac{\epsilon a_1(-(\beta\nu + a_2 - 1)a_1 - ((\beta-1)a_2 - 2\beta + 1)a_3 + \sqrt{W})}{((-\beta+1)a_2 + (\beta+1)(\beta\nu-1))a_1 + (\beta-1)(-a_3(\beta-1)a_2 + \sqrt{W} + a_3)} \\
b =& \frac{\beta(F+\sqrt{W})}{E}\left(\epsilon\left(2(GY(a_2-1)a_3 - \frac{\nu\beta + a_2 - 1}{2})(\beta\nu-1)a_1^2\right.\right. \\
& + (-2GY(\beta-1)(a_2-1)a_3^2 + (-(\beta-1)a_2^2 + (2\beta^2\nu - 2)a_2 - \nu\beta + 1)a_3 - \sqrt{W}(\beta\nu-1))a_1 \\
& \left.+a_2a_3((-1 + (-beta+1)a_2)a_3 + \sqrt{W})(\beta-1)\right) \\
& + \left((\beta\nu + a_2 - 1)(GY-1)(\beta\nu-1)a_1^2\right. \\
& + (((-\nu(GY-1)\beta^2 + \nu(GY-1)\beta)a_2 - (GY-1)\beta(\beta\nu-1))a_3 + \sqrt{W}(GY-1)(\beta\nu-1))a_1 \\
& \left.-(GY-1)a_3((-1 + (-\beta+1)a_2)a_3 + \sqrt{W})(\beta-1)\right) \\
r =& \frac{\beta\nu(U-\sqrt{W})}{M}\left(\epsilon\left(\frac{(-\beta\nu+1)a_1 + a_3(\beta-1)a_2}{2}\sqrt{W}\right.\right. \\
& + \left(G(a_2-1)a_3 - \frac{\nu\beta + a_2 - 1}{2}\right)(\nu\beta-1)a_1^2 \\
& - a_1a_3\left(G(\beta-1)(a_2-1)a_3 - \nu a_2\beta^2 + \frac{a_2^2+\nu}{2}\beta - \frac{(a_2-1)^2}{2}\right) \\
& \left.-\frac{a_3^2a_2(\beta-1)(\beta a_2 - a_2 + 1)}{2}\right) \\
& + \left(\frac{(\beta\nu-1)(G-1)a_1 - (\beta-1)(G-1)a_3}{2}\sqrt{W}\right. \\
& + \frac{(\nu\beta + a_2 - 1)(G-1)(\nu\beta-1)a_1^2}{2} \\
& - a_1a_3\left(\frac{\nu((G-1)a_2 + G - 1)\beta^2}{2} + \frac{(-\nu(G-1)a_2 - G + 1)\beta}{2}\right) \\
& \left.+\frac{a_3^2(\beta-1)(\beta a_2 - a_2 + 1)(G-1)}{2}\right)
\end{aligned}
\tag{30}
$$

where

$$W = (a_1\nu - a_2a_3)^2\beta^2 + 2(a_2-1)(a_1-a_3)(a_1\nu + a_2a_3)\beta + (a_2-1)^2(a_1-a_3)^2$$

$$E = 4((a_1\nu - a_3)\beta - a_1 + a_3)a_3(a_2-1)((a_2-\nu)\beta - a_2 + 1)Ga_1(Y-1)$$

$$F = (-\beta\nu - a_2 + 1)a_1 + (1 + (\beta-1)a_2)a_3$$

$$M = 2((\beta\nu-1)a_1 - a_3(\beta-1))a_3(a_2-1)((a_2-\nu)\beta - a_2 + 1)Ga_1(Y-1)$$

$$U = (\beta\nu + a_2 - 1)a_1 - a_3(\beta a_2 - a_2 + 1)$$

The solutions for E3 are too complex to draw any conclusions about feasibility requirements, so we will try to find it out by analysing and comparing the other steady states conditions.

A sample graph of the non-dimentional system's steady states derived from original system with influent nitrate concentration $N_o = 600\mu$M is shown in Figure 16.

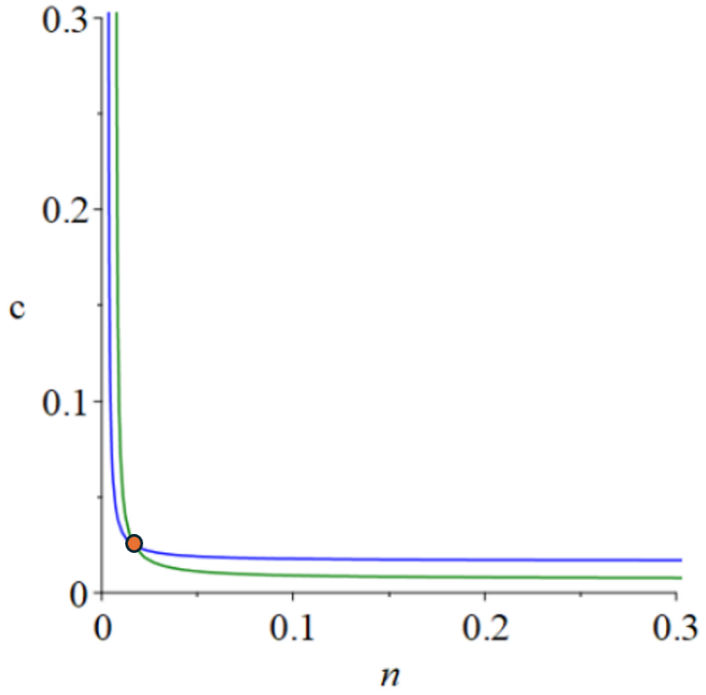


Figure 16: Steady states for the non-dimentional system; blue curve shows "b only" state E1, green curve shows "r only" state E2, and the coexistence steady state E3 is shown with orange dot at two curves intersection.

3.2.2 Stability analysis

To find the stability conditions, we compute the eigenvalues for each steady state.

1. E0 It is stable if

$$\begin{aligned}(\beta\nu - 1) &< a_2 a_3 \epsilon^2 + a_2\epsilon + a_3\epsilon \\ (\beta - 1) &< a_1\epsilon^2 + a_1\epsilon + \epsilon.\end{aligned} \tag{31}$$

As it was discussed in Section 3.2, values β and $\beta\nu$ show the ratio between the dilution rate and the corresponding bacteria growth rate. For a bacterium to survive (overgrow the dilution rate), we

generally expect ($\beta > 1$) and ($\beta\nu > 1$). The conditions for the degenerate steady state to be stable shown in (31) give a specific benchmark for each species survival.

In terms of the dimensional system (12), those conditions are:

$$\begin{aligned}(\mu_{R,max} - D) &< \frac{K_{RN}K_{RC}D}{N_oC_o} + \frac{K_{RN}D}{N_o} + \frac{K_{RC}D}{C_o} \\ (\mu_{B,max} - D) &< \frac{K_{BN}K_{BC}D}{N_oC_o} + \frac{K_{BN}D}{N_o} + \frac{K_{BC}D}{C_o}\end{aligned} \tag{32}$$

2. for "b only" E1 steady state, computation of eigenvalues is very complex, even with all variable values limited to O(ϵ). To find the conditions for E1 stability, we only analyzed the stability conditions for the terms of O(1) and O(ϵ) in each eigenvalue, assuming that with increasing order of ϵ the corresponding terms are too small to influence the whole expression's sign.

   (a) E1a steady state is stable if

   $$\epsilon(\beta\nu - 1) < a_2\epsilon(\beta - 1) \tag{33}$$

   In terms of the dimensional system 12,

   $$K_{BN}(\mu_{R,max} - D) < K_{RN}(\mu_{B,max} - D) \tag{34}$$

   This condition can be interpreted in terms of each species efficiency in processing a substrate. K_{BN} and K_{RN} are affinity (half saturation) constants on nitrate for the corresponding bacterium, $(\mu_{R,max} - D)$ and $(\mu_{B,max} - D)$ are the effective maximum growth rate that shows by how much each bacterium growth exceeds the dilution rate of the system. So, eventually expression $K_{BN}(\mu_{R,max} - D) < K_{RN}(\mu_{B,max} - D)$ compares each bacterial species efficiency in processing nitrate. If B is more efficient, a "b only" steady state E1a is stable.

   (b) E1b steady state is stable

   $$a_3\epsilon(\beta - 1) > a_1\epsilon(\beta\nu - 1) \tag{35}$$

   or, in term of the dimensional system

   $$K_{BC}(\mu_{R,max} - D) < K_{RC}(\mu_{B,max} - D) \tag{36}$$

accordingly, if species B is more efficient in processing organic carbon, a "b only" state E1b is stable.

The suggested interpretation agrees with the previous comment about each steady states solution's dependence/not dependence on the influent ratio: when two species compete for limited resources, then the ability to process each resource more efficiently decides the winner. Hence, we can conclude that E1a describes an steady state under n limiting condition, and E1b describes the steady state under c limiting conditions.

3. For E2 stability analysis, we used the same approach as for E1.

   (a) E2a steady state is stable if

   $$\epsilon(\beta\nu - 1) > a_2\epsilon(\beta - 1) \tag{37}$$

   or, in terms of the dimensional system 12

   $$K_{BN}(\mu_{R,max} - D) > K_{RN}(\mu_{B,max} - D) \tag{38}$$

   (b) E2b steady state is stable when

   $$a_3\epsilon(\beta - 1) < a_1\epsilon(\beta\nu - 1) \tag{39}$$

   or, in term of the dimensional system

   $$K_{BC}(\mu_{R,max} - D) > K_{RC}(\mu_{B,max} - D) \tag{40}$$

   We can say the E2a describes an r only steady state under n limiting conditions, and E2b - under c limiting conditions.

4. computation of the eigenvalues or their stability conditions for E3 turned out to be too complex to perform, so we could only draw conclusions based on other steady states behaviour. More specifically, we assume that both species could stably coexist only if any other steady state is not possible and/or not stable. Accordingly, if we find such conditions that none of E0, E1 and E2 are feasible or stable, we would expect E3 to emerge. We will look into the coexistence steady state possibility and stability in more detail in the next section.

3.2.3 Possibility and stability conditions for the coexistence steady state E3

To see the connection between E1, E2, and E3 steady states, we will have a closer look at their feasibility and stability shown in Table 2. To make it easier to see the connection of each set of conditions with the system parameters, instead of $a_i\epsilon$ notation, we will use k_{xy} as it was shown in (19).

Table 2: Comparison and possible combinations of feasibility and stability conditions for steady states "b only" E1 and "r only" E2.

steady state feasibility stability	E1a $\beta > 1 + k_{bn}$ $G > \frac{\beta-1}{\beta-1+k_{bc}}$ $k_{bn}(\beta\nu - 1) < k_{rn}(\beta - 1)$	E1b $\beta > 1 + k_{bc}$ $0 < G < \frac{\beta-1}{\beta-1-k_{bc}}$ $k_{rc}(\beta - 1) > k_{bc}(\beta\nu - 1)$	E2a $\beta\nu > 1 + k_{rn}$ $GY > \frac{\beta\nu-1}{\beta\nu-1+k_{rc}}$ $k_{bn}(\beta\nu - 1) > k_{rn}(\beta - 1)$	E2b $\beta\nu > 1 + k_{rc}$ $0 < GY < \frac{\beta\nu-1}{\beta\nu-1-k_{rc}}$ $k_{rc}(\beta - 1) < k_{bc}(\beta\nu - 1)$
E1a $\beta > 1 + k_{bn}$ $G > \frac{\beta-1}{\beta-1+k_{bc}}$ $k_{bn}(\beta\nu - 1) < k_{rn}(\beta - 1)$	not enough information to describe full system	same as E1a+E1b	same as E1a+E2a	same as E1a+E2b
E1b $\beta > 1 + k_{bc}$ $0 < G < \frac{\beta-1}{\beta-1-k_{bc}}$ $k_{rc}(\beta - 1) > k_{bc}(\beta\nu - 1)$	E1a+E1b, b only $\beta > \max(1 + k_{bn}, 1 + k_{bc})$ $G > 0$ Stability E1a and E1b combined	not enough information to describe full system	same as E1b+E2a	same as E1b+E2b
E2a $\beta\nu > 1 + k_{rn}$ $GY > \frac{\beta\nu-1}{\beta\nu-1+k_{rc}}$ $k_{bn}(\beta\nu - 1) > k_{rn}(\beta - 1)$	incompatible stability conditions	E1b+E2a, coexistence $\beta\nu > 1 + k_{rn}$ and $\beta > 1 + k_{bc}$ $0 < GY < \frac{\beta\nu-1}{\beta\nu-1+k_{rc}}$ $G > \frac{\beta-1}{\beta-1-k_{bc}}$ and $Y < 1$ Stability E2a and E1b combined	not enough information to describe full system	same as E2a+E2b
E2b $\beta\nu > 1 + k_{rc}$ $0 < GY < \frac{\beta\nu-1}{\beta\nu-1-k_{rc}}$ $k_{rc}(\beta - 1) < k_{bc}(\beta\nu - 1)$	E1a+E2b, coexistence $\beta > 1 + k_{bn}$ and $\beta\nu > 1 + k_{rc}$ $GY > \frac{\beta\nu-1}{\beta\nu-1-k_{rc}}$ $0 < G < \frac{\beta-1}{\beta-1+k_{bc}}$ and $Y > 1$ stability E2b and E1a combined	incompatible stability conditions	E2a+E2b, r only $\beta\nu > \max(1 + k_{rn}, 1 + k_{rc})$ $GY > 0$ Stability E2a and E2b combined	not enough information to describe full system

The first row and first column of Table 2 give a concise summary of each steady state's feasibility and stability conditions, and lower diagonal entries show the possible combinations - the conditions that do not exclude each other and hence can theoretically be combined in the a system configuration. Diagonal cells only describe system's functionality under one substrate limitation so they are not providing enough information for the full system description.

Combinations E1a+E2a and E1b+E2b are not possible as in each pair the stability conditions are the reverse of each other.

Configuration E1a+E1b is possible (shaded in blue), but since both E1 steady states describe a "b

only" system, we can expect that only one species (species b) would survive in a system that satisfy all those requirements. Such combination would just show that species b is more efficient in processing both substrates, so it pushes its competitor, species r, to extinction. Then, depending on the actual influent, specific outcome can be of type E1a or E1b.

Similarly, configuration E2a+E2b is possible (shaded in green), and it will describe a system in which only one species, in this case species r, would survive, so that depending on the specific influent concentration, either E1a or E2b is the actual system's outcome.

There are two configurations that promise a possibility of both species coexistence: E1b+E2a and E1a+E2b.

E1b+E2a means that b is more efficient in processing n, and r is more efficient in processing c. Combining both feasibility we have $\beta > 1 + k_{bc}$ and $\beta\nu > 1 + k_{rn}$. However, for a coexistence to happen, we would need that "one only" species ("r only" or "b only") steady state was not possible, so we assume that $0 < GY < \frac{\beta\nu-1}{\beta\nu-1+k_{rc}}$ so that E2a is not feasible, and $G > \frac{\beta-1}{\beta-1-k_{bc}}$ so that E1b in not feasible. This combination of conditions is not incompatible; even more, from the fact that $\frac{\beta\nu-1}{\beta\nu-1+k_{rc}} < 1$ and $\frac{\beta-1}{\beta-1-k_{bc}} > 1$ we see that it can happen if $Y < 1$ so this requirement is added to the feasibility requirements. The list of feasibility conditions for a coexistence to emerge for system configuration E1b+E2a is

1. $\beta > 1 + k_{bc}$
2. $\beta\nu > 1 + k_{rn}$
3. $0 < GY < \frac{\beta\nu-1}{\beta\nu-1+k_{rc}}$
4. $G > \frac{\beta-1}{\beta-1-k_{bc}}$
5. $Y < 1$

We can expect that under conditions satisfying all those requirements a system with general configuration E1b+E2a can produce a stable coexistence of two bacterial species. The actual outcome of such a system will depend on the specific influent concentration: either "r only" E2a, or "b only" E1b, or a coexistence steady state E3. However, at this point we cannot specify which E3 variation, a or b, can appear in such system.

For the combination E1a+E2b, b is more efficient in processing n, r is more efficient in processing c. Using the same logic, we can find the feasibility conditions for a two species coexistence in this case:

1. $\beta > 1 + k_{bn}$

2. $\beta\nu > 1 + k_{rc}$

3. $GY > \frac{\beta\nu-1}{\beta\nu-1-k_{rc}}$

4. $0 < G < \frac{\beta-1}{\beta-1+k_{bc}}$

5. $Y > 1$

Hence, we can expect that a system with a general configuration E1a+E2b, can produce either "b only" E1a, or "r only" E2b, or a stable coexistence, depending on the actual influent concentrations.
To see which variation of E3 steady state appears in each coexistence we ran simulations for two sample systems that satisfy all requirements found for E1a+E2b and E1b+E2a configurations. The influent ratio in each case varies so we can see the whole spectrum of the systems outcomes under different initial conditions.

System possible outcomes for a E2a+E1b configuration are shown in Figure 17:

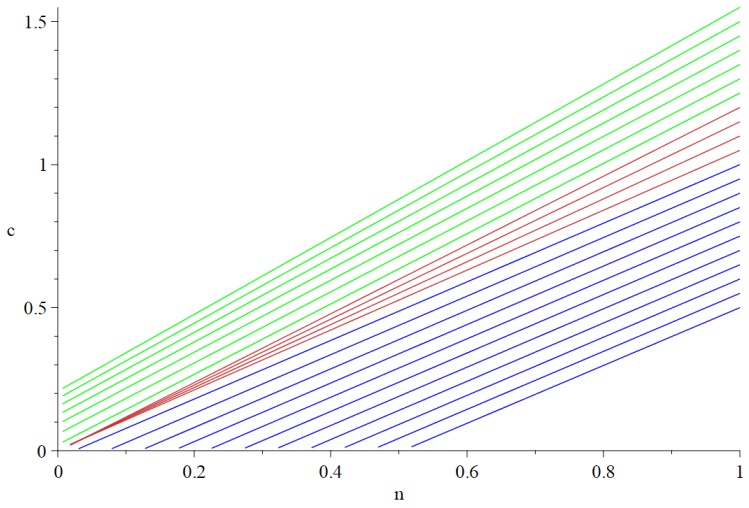


Figure 17: Sample system trajectories with different influent ratio k for a E1b+E2a configuration. "r only" steady state E2a (possible trajectories shown in green) appears when n is a limiting substrate, and "b only" E1b (possible trajectories shown in blue) appears when c is a limiting substrate. Red lines show possible trajectories leading to coexistence steady state.

As we expected, E2a "r only" appear when the system is under n limiting conditions, E1b "b only" appears when system is under c limiting conditions. For this system's configuration, coexistence steady state E3b appears when the corresponding requirements for the system's parameters are satisfied.
Simulation results for a sample system of type E1a+E2b shown in Figure 18:

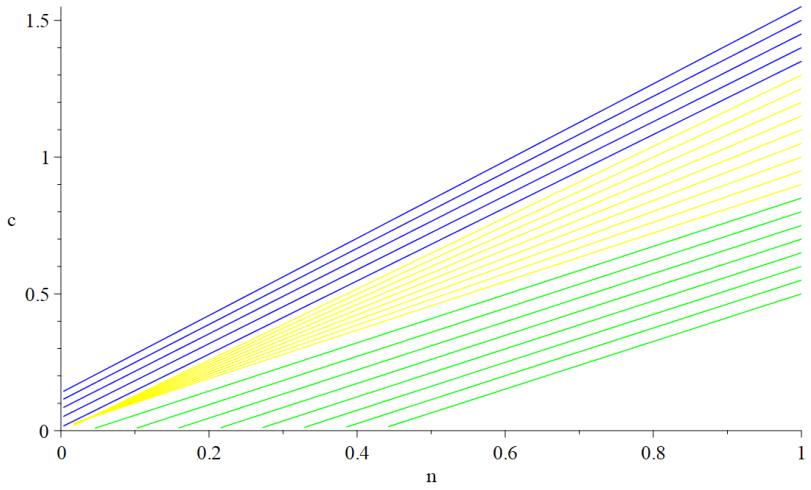


Figure 18: Sample dynamics for a system of configuration E1a+E2b with different initial k ratio. "r only" E2b (possible trajectories shown in green) appears when c is a limiting substrate, and "b only" E1a (possible trajectories shown in blue) appears when n is a limiting substrate. Yellow lines show possible trajectories leading to coexistence.

For a E1a+E2b configuration, "r only" E2b steady state appear when c is a limiting substrate, and "b only" E1a steady state appears when n is a limiting substrate. In this case, solution steady state E3a appears for coexistence outcomes.

Using those results and knowing parameters for two bacterial species we can predict if they potentially can coexist and design the system settings that would lead to a coexistence outcome.

In the next section, we run simulation for model (9) and (12) with parameters outlined in Table 1 to see how simulations outcome relate to the experimental data reported in the literature and compare the performance for both models.

3.3 A comparison between model with Liebeg's minimum principle and and model with two Monod terms in the growth rate definition

Table 3 shows the influent and effluent concentrations measured in the series of experiments described in [49] and [48] that we are going to use for simulations to see how the model's output agrees with the experimental data.

Table 3: Influent concentration, observed competition outcomes, measured biomass concentrations and substrates effluent concentrations at steady states in chemostat enrichment cultures reported in [48] - Case Study 1, and [49] - Case Study 2.

	influent			Competition	Biomass concentration			Effluent	
	Acetate	Nitrate	Ratio	outcome	DEN	DNRA	Total	Acetate	Nitrate
Case Study 1	22050	11790	1.87	DNRA dominance	86	8465	8551	4600	30
	17690	11790	1.5	DNRA dominance	87	8655	8742	30	30
	14500	11790	1.23	Coexistence	1510	4529	6039	30	30
	13680	11790	1.16	Coexistence	2082	3396	5478	30	30
	12730	11790	1.08	Coexistence	2965	3489	6445	30	30
	10969	11790	0.93	Coexistence	4042	713	4755	30	30
	7780	11790	0.66	DEN dominance	3601	0	3601	30	3700
Case Study 2	2616	6643	0.39	DEN dominance	n/a	n/a	1341	n/a	n/a
	4356	5857	0.74	DEN dominance	n/a	n/a	n/a	n/a	n/a
	5152	5857	0.88	DEN dominance	n/a	n/a	1667	n/a	n/a
	6278	5857	1.07	DEN dominance	n/a	n/a	2439	n/a	n/a
	9866	5857	1.68	DNRA dominance	n/a	n/a	3659	n/a	na/

All concentration values are in μM. Acetate was used for organic carbon substrate. Influent ratio represents Acetate/Nitrate. DEN is used instead of "denitrifiers".

Effluent concentrations were not reported explicitly by the original researches, and the values shown in the table were obtained from a graph by using an online digitizer tool [20], so they may not fully reflect the accuracy of the experiment.

Figure 19 shows both models' steady states:

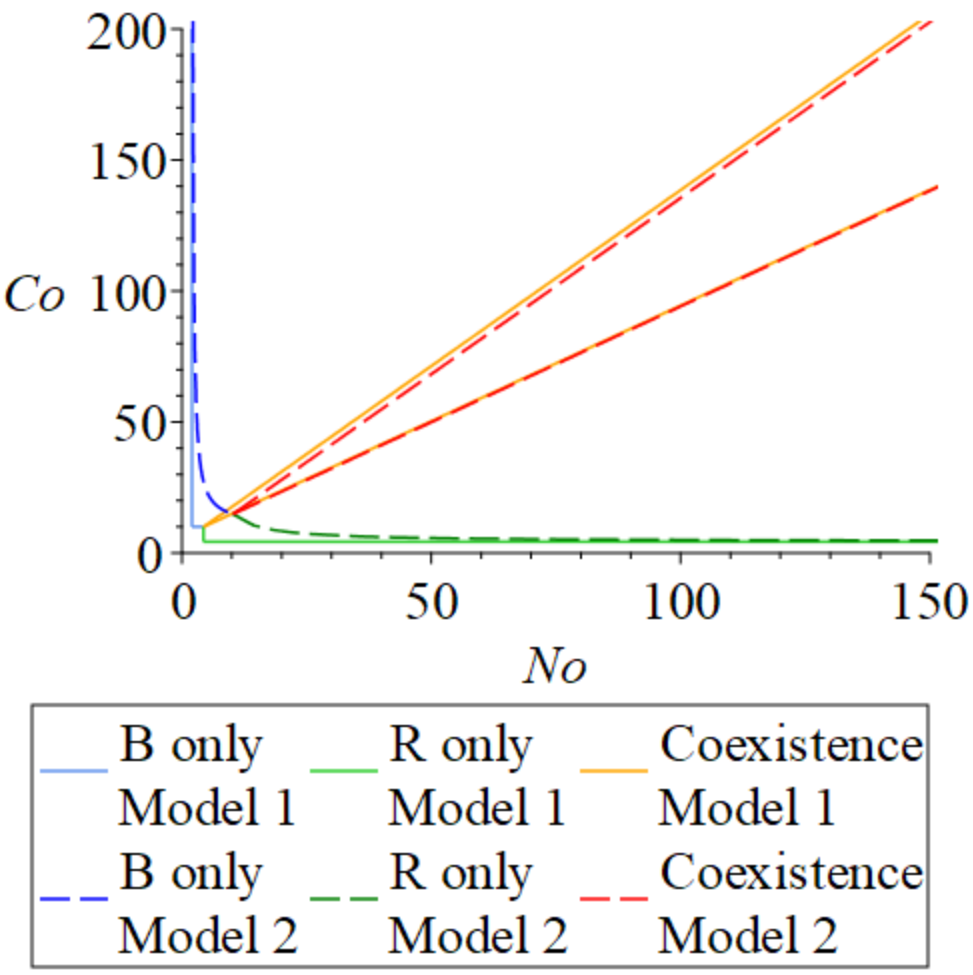


Figure 19: steady states found for model (9), referred to as Model 1, and model (12), referred to as Model 2.

As we can see in Figure 19, the main difference is in the predicted outcomes for small influent concentrations and the coexistence values for N and C, even though they are not far apart. Also, the upper limit of IC leading to coexistence is slightly higher for Model 1 (9). For large influent concentrations when system is at saturation, the predicted outcome should be very similar.

A system having parameters shown in Table 1 has E1a+E2b configuration. Accordingly, depending on the influent concentrations, the possible outcome would be E1a"b only" steady state under n limitations, or E2b "r only" under c limitations, or E3a coexistence steady state. Figure 20 shows the the result of simulation with model (12) done with Case Study 1 influent values.

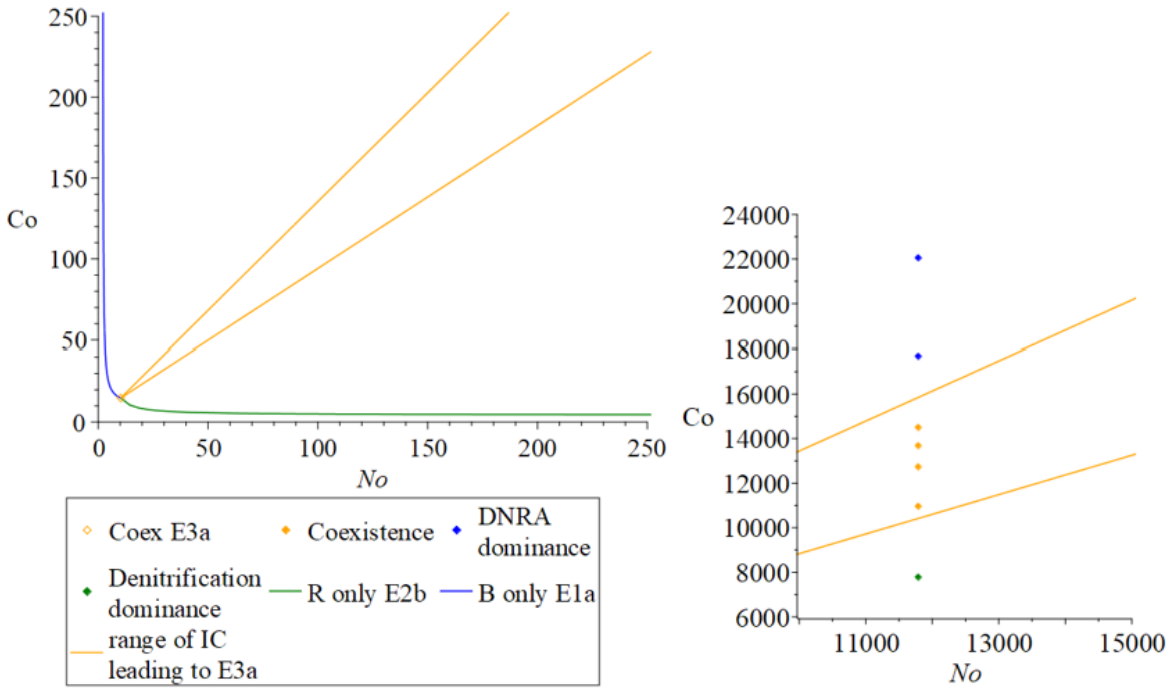


Figure 20: Model (12) application to Case Study 1. Blue points show the initial condition of experiments resulting in DNRA domination, green point shows the initial condition of the experiment resulting in denitrifiers' domination, and orange points show the initial conditions leading to both species coexistence.

Blue points show the experiments that resulted in observed DNRA domination, green points show the experiments resulting in denitrification domination, and orange points show the resulting coexistence. We can see that the model's prediction matches the experimental data.

Now, we run simulations on the system (9) analysed in Chapter 2 with the same initial conditions to compare the models' performance, the results are shown in Figure 21:

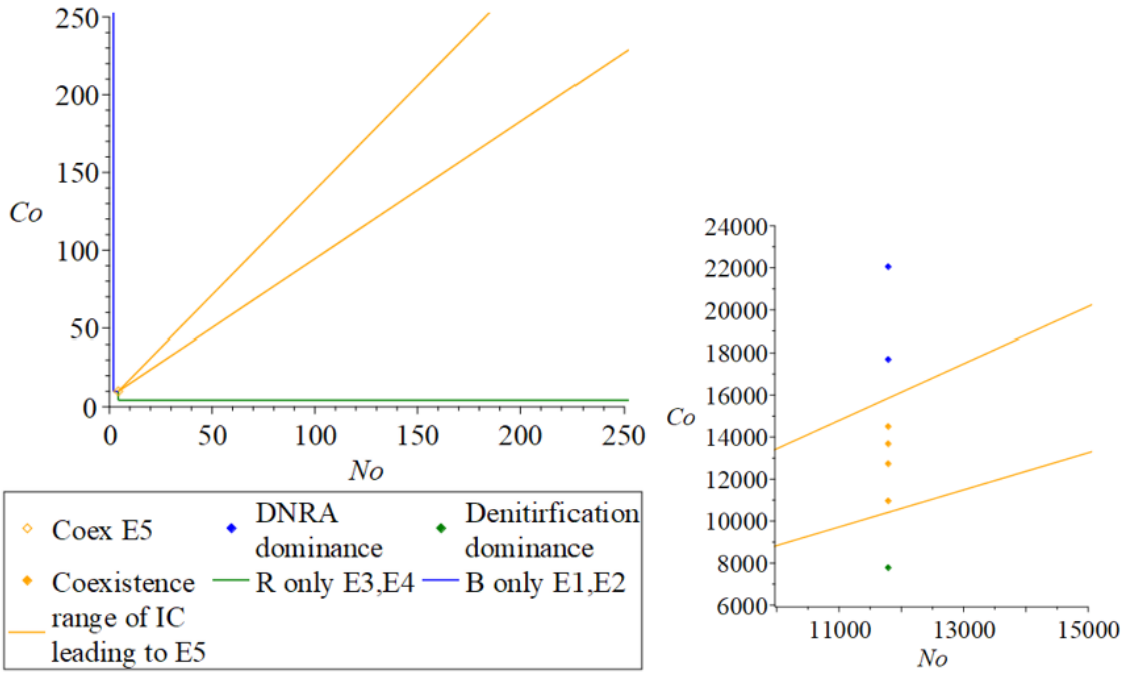


Figure 21: Model (9) application to Case Study 1. Blue points show the IC of experiments resulting in DNRA domination, green point shows the IC of the experiment resulting in denitrifiers' domination, and orange points show the IC leading to both species coexistence.

As we can see, both models classify the cases in the same way, matching the experiments' results.

We will now look into the final values measured in the experiments and the values returned by each model's simulation to see how accurate the models' predictions are. Table 4 show the numerical simulations results for model (9) considered in chapter 2 (Model 1) and model (12) analysed in the current chapter (Model 2).

Table 4: Simulation results for Case Study 1 for Model 1 (9) and Model 2 (12)

	Influent concentrations, μM		C_o/N_o	Biomass concentrations, μM		Effluent concentrations, μM		
	N_o	C_o	k	R	B	N	C	Outcome
Experiment 1	11790	22050	1.8702	86	8465	30	4600	DNRA dominance
Model 1				10^{-6}	7733	2	6204	B only E2
Model 2				10^{-6}	7733	2	6204	B only E1a
Experiment 2	11790	17690	1.5004	87	8655	30	30	DNRA dominance
Model 1				10^{-6}	7733	2	1844	B only E2
Model 2				0.156	7733	2	1844	B only E1a
Experiment 3	11790	14500	1.2298	1510	4528	30	30	Coexistence
Model 1				1265	5806	4	10	Coex E5
Model 2				1262	5807	10	14	Coex E3a
Experiment 4	11790	13680	1.160	2082	3396	30	30	Coexistence
Model 1				2031	4640	4	10	Coex E5
Model2				2028	4640	10	15	Coex E3a
Experiment 5	11790	12730	1.0797	2965	3480	30	30	Coexistence
Model 1				2919	3288	4	10	Coex E5
Model 2				2916	3288	10	14	Coex E3a
Experiment 6	11790	10960	0.9296	4042	713	30	30	Coexistence
Model 1				4574	770	4	10	CoexE5
Model 2				4571	770	10	14	Coex E3a
Experiment 7	11790	7780	0.65988	3601	0	3700	30	Denitrification dominance
Model 1				3795	10^{-6}	2986	4	R only E3
Model 2				3795	10^{-25}	2984	4	R only E2b

.

B and R stand for DNRA and denitrifying bacteria correspondingly. N and C represent nitrate and acetate correspondingly.

Lines highlighted in gray show the experimental data, lines highlighted in blue show the simulation data from model (9) analysed in chapter 2 (referred as Model 1), lines highlighted in light brown show the simulation data from model (12) analysed in this chapter (Model 2).

Simulation results were in most cases rounded to the nearest integer. Values for the biomass concentrations computed by both models are very close and align reasonably well with the experimentally measured quantities. The effluent concentrations obtained from both models simulations are also quite close to each other and reflect the dynamics of the experimental results in most cases, except for acetate effluent concentration shown in Experiment 2 where the experimental data shows a small value 30 μM while both models return march larger numbers. However, as it was mentioned before, the effluent concentrations values were not reported explicitly in the original source, and the values shown in the table were obtained from a graph

by a plot digitizer tool, so they might not fully reflect the actual experiments outcome. Unfortunately, without additional information it is not possible to speculate about a reason for this discrepancy. Overall, a more accurate measurements of the effluent nitrate and organic carbon concentration would be necessary to validate the Model 1 and Model 2 predictions.

Now we apply both models to Case Study 2 shown in the lower part of table 3. In this series of experiment there is no data for effluent nitrate and organic carbon concentrations, nor for each species bacterium concentration, only data for influent concentration and total biomass concentration is available. However, after each experiment a conclusion was drawn about denitrification or DNRA dominance.

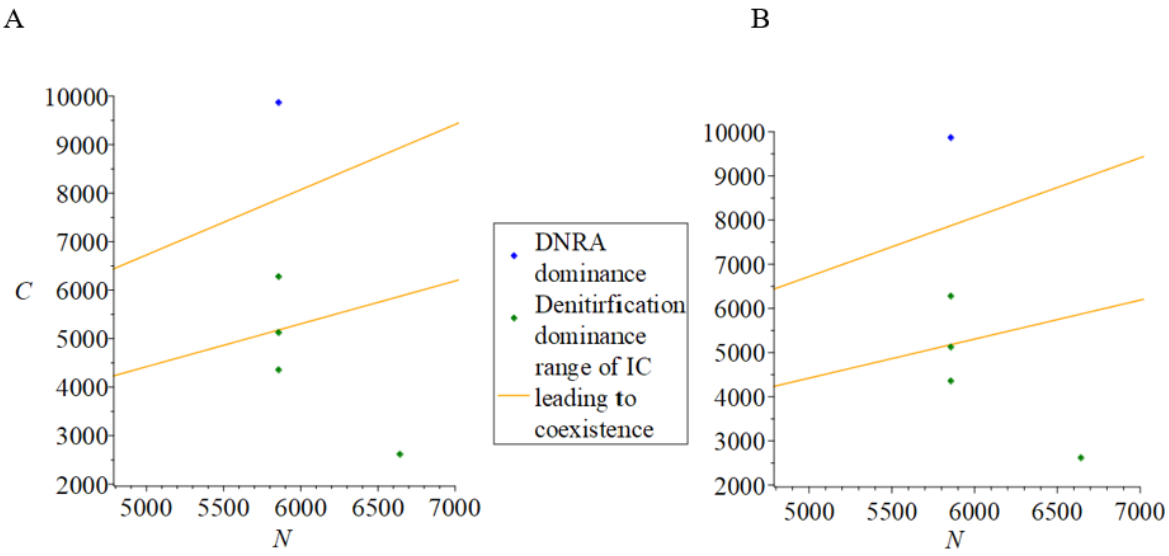


Figure 22: Models application to Case study 2. Graph A shows results for Model 1, and graph B shown results for Model 2. Blue points show the IC of experiments resulting in DNRA domincance, green point show the IC of the experiments resulting in denitrification dominance.

As we can see both models return identical results, with four predictions coinciding with the experiment results, and one experimental outcome classified into coexistence steady state, while the experiment is classified as showing the dominance for denitrification.

We will now compare the numerical results from the simulation and the experiments. Table 5 shows the simulation results for Case Study 2:

Table 5: Simulation results for Case Study 2 for Model 1 and Model 2.

	Influent concentrations (μM)		C_o/N_o	Biomass concentrations (μM)		Total biomass (μM)	Outcome
	N_o	C_o	k	R	B		
Experiment 1	6643	2616	0.40	n/a	n/a	1341	Denitrification dominance
Model 1				1274	10^{-6}	1274	R only E3
Model 2				1274	10^{-6}	1274	R only E2b
Experiment 2	5857	5125	0.88	n/a	n/a	1667	Denitrification dominance
Model 1				2499	10^{-6}	2498	R only E3
Model 2				2498	10^{-5}	2498	R only E2b
Experiment 3	5857	6278	1.07	n/a	n/a	2439	Denitrification dominance
Model 1				1495	1563	3058	Coex E5
Model 2				1492	1564	3056	Coex E3a
Experiment 4	5857	9866	1.68	n/a	n/a	3659	DNRA dominance
Model 1				10^{-7}	3841	3841	B only E2
Model 2				10^{-7}	3841	3841	B only E3a

B and R stand for DNRA and denitrifying bacteria correspondingly. N and C represent nitrate and acetate correspondingly.

Fore Case Study 2, there is no data for each bacteria concentration, only the total biomass concentration, so we compare the total biomass predicted by each model. We ignore the experiment that does not show any numerical values.

Both models prediction line up very well with the data shown for Experiment 1 and Experiment 4. In both cases, influent concentrations are far from the possible coexistence area (see graphs in Figure 22), and the system clearly lead to a one species only steady state and corresponding computation closely match the experimental outcome.

Experiments data shown in Experiment 2 and Experiment 3 however differ considerably from the predictions. More specifically, Experiment 3 was originally qualified and Denitrification dominance, while both models predict two species coexistence. To investigate the situation, we have looked into the article where the experimental data was originally reported, [49].

The original experiment had the goal to show that nitrate limitation is the dominant factor in selecting DNRA able bacteria over denitrifiers. The experiment was set up as an incremental change of the chemostat conditions from acetate (organic carbon source) limitation suitable for denitrifiers, to nitrate limitation that

hypothetically should support emergence of the DNRA able population. The measurements shown in Table 3 were done at different stages of the system conversion from denitrification dominance to DNRA dominance.

Accordingly, the option of denitrifiers and DNRA able bacteria coexisting was not even considered. As for the data reported in Experiment 4 in Table 5, it refers to the a stage of experiment that lasted for 74 days, when the influent concentrations were changed incrementally and the bacterial populations were adjusting along. The original paper did not specify at what day the biomass and effluent concentrations were measured, but gene PCR that they show (see Figure 1 in [49]) gives evidence that both denitrifiers and DNRA bacteria were present in the culture at the end of the experiment. However, since complete shift to DNRA dominance in the culture had not happened at this stage, the experimental outcome was labeled as denitrification dominance.

This information actually supports the models' prediction that a coexistence should be expected for the influent concentration shown in Experiment 4. Numerically, the predicted quantity and the reported number align reasonably well showing about 20% difference.

There is more discrepancy between the reported and predicted numbers for Experiment 2. This influent concentration lays at the very border of the coexistence range, and there might be two possible reasons for the difference:

1. since we do not know at what specific point the bacterium population was sampled in this case, and the setting of the experiment assumes that the population shifts steadily, the sampling might be done before (or after) the steady state settled, and this causes a larger discrepancy;

2. models perform better in the "clear" cases when an initial conditions are clearly in the area leading to a specific steady state, but the predictions might be less accurate in case of "marginal" situations, when influent concentration is at the "border" between two zones.

In both cases, additional data is required to clarify the reason of the discrepancy.

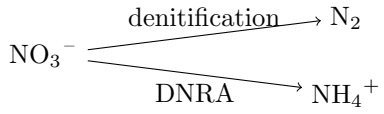
3.4 Summary

In Chapter 3, we considered a more realistic model (12) and performed its analysis. We found the system's steady states and identified feasibility and stability conditions. We described four possible system configurations and clarify the systems' parameters that can lead to both bacterial species coexistence. Lastly, we applied our results to experimental data and show how the predictions relate to the reported values.
We saw that the models introduced in Chapter 2 (9) and the model analysed in Chapter 3 (12) return

similar results, but model (12) can be analysed with standard mathematical methods. Due to this analysis we were able to find more general connections between system's parameters value and expected outcomes (configurations) and deduce the conditions leading to two species coexistence.

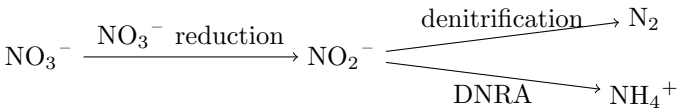
4 Chapter 4: Model for denitrification and DNRA competition with three bacterial species

Both systems we analysed so far were built with an assumption that both denitrification and DNRA reactions are performed completely by a corresponding bacteria, so model includes a one step reaction in each case:

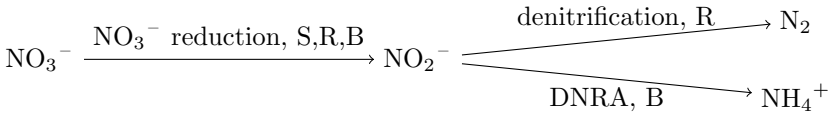


However, as it was discussed in Section 1.2.2, in many cases soil bacteria lack one or more enzymes necessary for the complete denitrification or DNRA, and hence they are only capable of performing some steps in the chain of nitrogen oxides reduction. As a result, a community of a few bacterial species is responsible for the complete denitrification or DNRA [25]. Modelling denitrification and DNRA as multi-steps reactions performed by a community of bacteria might be very helpful is understanding those bacteria connections. Successful coexistence of such bacteria is a key to reducing by-products of a truncated denitrification, such as NO and N_2O [52], [25].

In this chapter, we will consider two step reactions - first reduction of NO_3^- to NO_2^-, and then nitrite reduction to the final product - N_2 or NH_4^+ for denitrification and DNRA correspondingly:



To reflect the idea of a community of bacterial species each performing one or more steps in the complete denitrification or DNRA, we will build a model with three bacterial species. The newly added species, S, is only able to perform the first step of reducing nitrate to produce nitrite. The reason for this choice is that bacteria performing only $NO_3^- \rightarrow NO_2^-$ step in the chain of nitrate reducing (NO_2^- accumulators in the denitrifiers' classification given in [33]) are very abundant and exceed the number of denitrifiers able to perform complete reation ([10],[21]). The other two bacteria, as before, are able to perform both steps:



In this way, all three species compete for nitrate, and species R and B complete for nitrite. We modify the

previous system to reflect those features:

$$\begin{aligned}
\frac{dN_1}{dt} &= (N_0 - N_1)D - \frac{\mu_S S}{Y_{SN}} - \frac{\mu_B B}{Y_{BN_1}} - \frac{\mu_R R}{Y_{RN_1}} \\
\frac{dN_2}{dt} &= \frac{\mu_S S}{Y_{SN}} + \frac{\mu_B B}{Y_{BN_1}} + \frac{\mu_R R}{Y_{RN_1}} - \frac{\mu_{B2} B}{Y_{BN_2}} - \frac{\mu_{R2} R}{Y_{RN_2}} - DN_2 \\
\frac{dC}{dt} &= (C_0 - C)D - \frac{\mu_S S}{Y_{SC}} - \frac{\mu_B B}{Y_{BC}} - \frac{\mu_R R}{Y_{RC}} - \frac{\mu_{B2} B}{Y_{BC}} - \frac{\mu_{R2} R}{Y_{RC}} \\
\frac{dS}{dt} &= (\mu_S - D)S \\
\frac{dB}{dt} &= (\mu_B - D)B \\
\frac{dR}{dt} &= (\mu_R - D)R
\end{aligned} \tag{41}$$

where N_1 and N_2 are nitrate and nitrite concentrations correspondingly, C is the organic carbon concentration, and S is the concentration of the bacteria reducing only $NO_3{}^-$ to $NO_2{}^-$, and B and R are concentrations of DNRA and denitrifying bacteria correspondingly. Y_{XN1} represents the yield for bacterium X when nitrate is used as a substrate, Y_{XN2} is the yield when nitrite is used as a substrate, and Y_{XC} is the yield for organic carbon. D represents the dilution rate. We now need to introduce two different growth rates definitions for species B and R and one definition for S:

$$\begin{aligned}
\mu_S &= \mu_{S,\max} \frac{N_1}{K_{SN} + N_1} \frac{C}{K_{SC} + C} \\
\mu_B &= \mu_{B,\max} \frac{N_1}{K_{BN} + N_1} \frac{C}{K_{BC} + C} \\
\mu_R &= \mu_{R,\max} \frac{N_1}{K_{RN} + N_1} \frac{C}{K_{RC} + C} \\
\mu_{B2} &= \mu_{B,\max} \frac{N_2}{K_{BN_2} + N_2} \frac{C}{K_{BC} + C} \\
\mu_{R2} &= \mu_{R,\max} \frac{N_2}{K_{RN_2} + N_2} \frac{C}{K_{RC} + C}
\end{aligned} \tag{42}$$

Finding steady states with a sample parameter set shows that we can expect the following types of steady states: 1) degenerate with all bacterial species extinct; 2) one species survival only, for each R, B, and S; 3) two species coexistence, for each pair - R and S, B and S, R and B; 4) three species coexistence.

We will discuss the strategy to the system analysis in the next section.

4.1 Model analysis

There are several difficulties associated with system (41) analysis. As it was mentioned in section 1.4, any models including explicit bacterial population dynamics have added complexity and increased uncertainty

due to uncertainties in the parameters. We see all of those issues appearing in the current model. Firstly, all computations are very complicated due to the system's complexity. Non-dimentionalizing the system and using approximations (as it was done in Chapter 3) do not help as the expressions are still too complex for analysis. Approximation to O(1) is possible but the results are not informative.

Another even more important problem, is finding/choosing the parameters values. Research over the species performing complete denitrification and DNRA first appeared decades ago so that now more results are available, and the bacteria's parameters are better known. However, there is much less literature on truncated denitrification and the corresponding bacterial species, which makes it much harder to find parameter value for the model.

Because of the difficulties in model complexity, we will forgo a traditional analysis in favor of an exploratory one through simulations and sensitivity analysis. Specifically, we will

1. run numerical simulations with different sets of parameters to have a general idea about the possible 2 and 3 species coexistence

2. explore the model's sensitivity to identify the parameters that have least influence on the system outcome and then investigate potential simplifications of the model to make it's analysis more feasible.

4.2 Numerical simulation and parameters choices

The main goal of numerical simulations is to see if three species coexistence is possible and what the conditions might be both in terms of the bacteria parameters and the the system settings.

Literature about microbial multi-species coexistence communities is quite extensive (a short review can be found in [41]), and the two main approaches in explaining its mechanisms can be summarised as follows [4]:

1. pairwise competitions of the species in a larger community defines the composition of complex communities. That basically means that only species that are able to stably coexist in an isolated two species environment can potentially coexist in a larger microbial communities,

2. coexistence in a multi-species community is more complex and cannot be defined just by the ability of each pair to coexist in an isolated system. Rather, multi-species coexistence emerges as a result of cooperation on different levels so that even species that cannot win in a pairwise competition can still be part of and even thrive in a larger community.

There is no consensus yet as to what approach is correct, and some researchers state that both might be true for the microbial communities of different types (see for example [4], [34], [18]).

Accordingly, we will use some more general considerations than a strict requirement of survival in a pairwise competition for the species in question. For our simulation, we chose the parameters based on the following principles:

1. no parameters for B and R that were used in models (9) and (12) are changed;
2. yield and affinity constants for B and R related to nitrite substrate should make its processing less efficient than nitrate;
3. we assume that yield for S on both substrates is similar to those of B and R;
4. we assume that affinity constants of the new species S should allow it to compete with each of the other species under some conditions;
5. we assume that the maximum growth rate of species S should not be smaller than the lowest maximum growth rate of each B and R.

The parameters used following these assumptions are listed in Table 6

Table 6: Parameter values used for simulations on 3 species model (41)

parameter	meaning	units	range/value
$\mu_{max,B}$	maximum growth rate for B	h^{-1}	0.052
Y_{BN1}	yield for unit of biomass of B per unit nitrate consumed	1	0.656
Y_{BN2}	yield for unit of biomass of B per unit nitrite consumed	1	0.6
Y_{BC}	yield for unit of biomass of B per unit COD consumed	1	0.488
K_{BN}	affinity constant for B to nitrate	μM	2
K_{BN2}	affinity constant for B to nitrite	μM	3
K_{BC}	affinity constant for B to COD	μM	10
$\mu_{max,R}$	maximum growth rate for R	h^{-1}	0.086
Y_{RN1}	yield for unit of biomass of R per unit nitrate consumed	1	0.431
Y_{RN2}	yield for unit of biomass of R per unit nitrite consumed	1	0.4
Y_{RC}	yield for unit of biomass of R per unit COD consumed	1	0.488
K_{RN1}	affinity constant for R to nitrate	μM	10
K_{RN2}	affinity constant for R to nitrite	μM	11
K_{RC}	affinity constant for R to COD	μM	10
$\mu_{max,S}$	maximum growth rate for S	h^{-1}	0.06..0.12
Y_{SN}	yield for unit of biomass of S per unit nitrate consumed	1	0.5
Y_{SC}	yield for unit of biomass of S per unit acetate consumed	1	0.488
K_{SN}	affinity constant for S to nitrate	μM	3
K_{SC}	affinity constant for S to COD	μM	8

Parameter values for R and B related to nitrate and carbon processing are the same as in Table 1 as they were used in Chapter 2 and Chapter 3 [48]. Parameter values for S and parameters related to processing nitrite for R and B are all assumed based on the criteria given before.

We have run simulations for a wide range of influent concentrations k and different $\mu_{max,S}$. The concise summary of simulations outcomes are shown in tables below.

Table 7: Simulations outcome for $\mu_{max,S} = 0.06\text{h}^{-1}$

k	1	1.2	1.4	1.6	1.8	2	2.2	2.4	2.6	2.8
R only	x	x	x							
B only									x	x
S only										
R & B coex				x	x	x	x	x		
R & S coex										
B & S coex										
R & B & S coex										

We consider a species X extinct if by the end of the simulation its biomass concentration $X < 10^{-4}\ \mu\text{M}$. Time frame for the simulations is 2000 hours.

In Table 7, top row shows the influent ratio value k used for the simulations, the possible outcomes are shown in the first column - those are one species only surviving, R, B, or S, two species coexistence, $R\&B$, $R\&S$ and $B\&S$, and three species coexistence. Cross in the corresponding cell marks the type of outcome appearing in the simulation.

Three species coexistence was not observed for $\mu_{max,S} = 0.06\ \text{h}^{-1}$, and the simulations outcomes are similar to two species system performance: for lower C/N ratio $1 \leq k < 1.6$ denitrifiers R dominate, for $1.6 \leq k < 2.6$ R and B coexist, and for $k \geq 2.6$ bacteria B dominates. It is interesting to note that R and B coexistence happens for a much wider range of k than in a two species system - in both models considered before, the coexistence range was approximately $0.88 \leq k \leq 1.344$. It seems that the presence of S, even though its concentration are very small, changes the survival range for other members of the community.

Table 8: Simulations outcome for $\mu_{max,S} = 0.07\text{h}^{-1}$

k	1	1.2	1.4	1.6	1.8	2	2.2	2.4	2.6	2.8
R only	x	x	x							
B only									x	x
S only										
R & B coex				x						
R & S coex										
B & S coex										
R & B & S coex					x	x	x	x		

As we can see in Table 8, slight increase in $\mu_{max,S}$ results in triple coexistence appearing for $1.8 \leq k < 2.6$, with two species $R\&B$ coexistence shown for $k = 1.6$. As it is expected, R dominating at lower influent ratio, $1 \leq k < 1.6$, and B dominates at higher ratios $k > 2.4$.

Table 9: Simulations outcome for $\mu_{max,S} = 0.09\text{h}^{-1}$

k	1	1.2	1.4	1.6	1.8	2	2.2	2.4	2.6	2.8
R only	x	x	x							
B only										x
S only										
R & B coex										
R & S coex										
B & S coex									x	
R & B & S coex				x	x	x	x	x		

For $\mu_{max,S} = 0.09$ h^{-1} (Table 9), the range of triple coexistence increased to $1.6 \leq k < 2.4$, and species B and S coexist in two species system at $k = 2.6$. As before, R dominates at smaller influent ratios $k < 1.6$, and B at higher $k \geq 2.8$.

Table 10: Simulations outcome for $\mu_{max,S} = 0.11\text{h}^{-1}$

k	0.4	0.6	0.8	k=1	1.2	1.4	1.6	1.8	2	2.2	2.4	2.6	2.8	3	3.2	3.4
R only																
B only																
S only																
R & B coex																
R & S coex	x	x	x	x	x	x	x									
B & S coex												x	x	x	x	x
R & B & S coex								x	x	x	x					

With $\mu_{max,S} = 0.11$ h^{-1} (Table 10), S can coexist with R in a two species system $R\&S$ starting from very small ratio, $0.4 \leq k < 1.8$, and with B in a two species system $B\&S$ for $2.6 \geq k$. All three species coexist $1.8 \leq k < 2.6$. Based on this results we can say that if S grows fast enough (in this case faster than each of R and B), it survives though all spectrum of influent ratios that we checked.

Figure 23 shows the simulations results for biomass concentration for $k = 1.8$ and $k = 2.2$, when simulations outcome show three species coexistence.

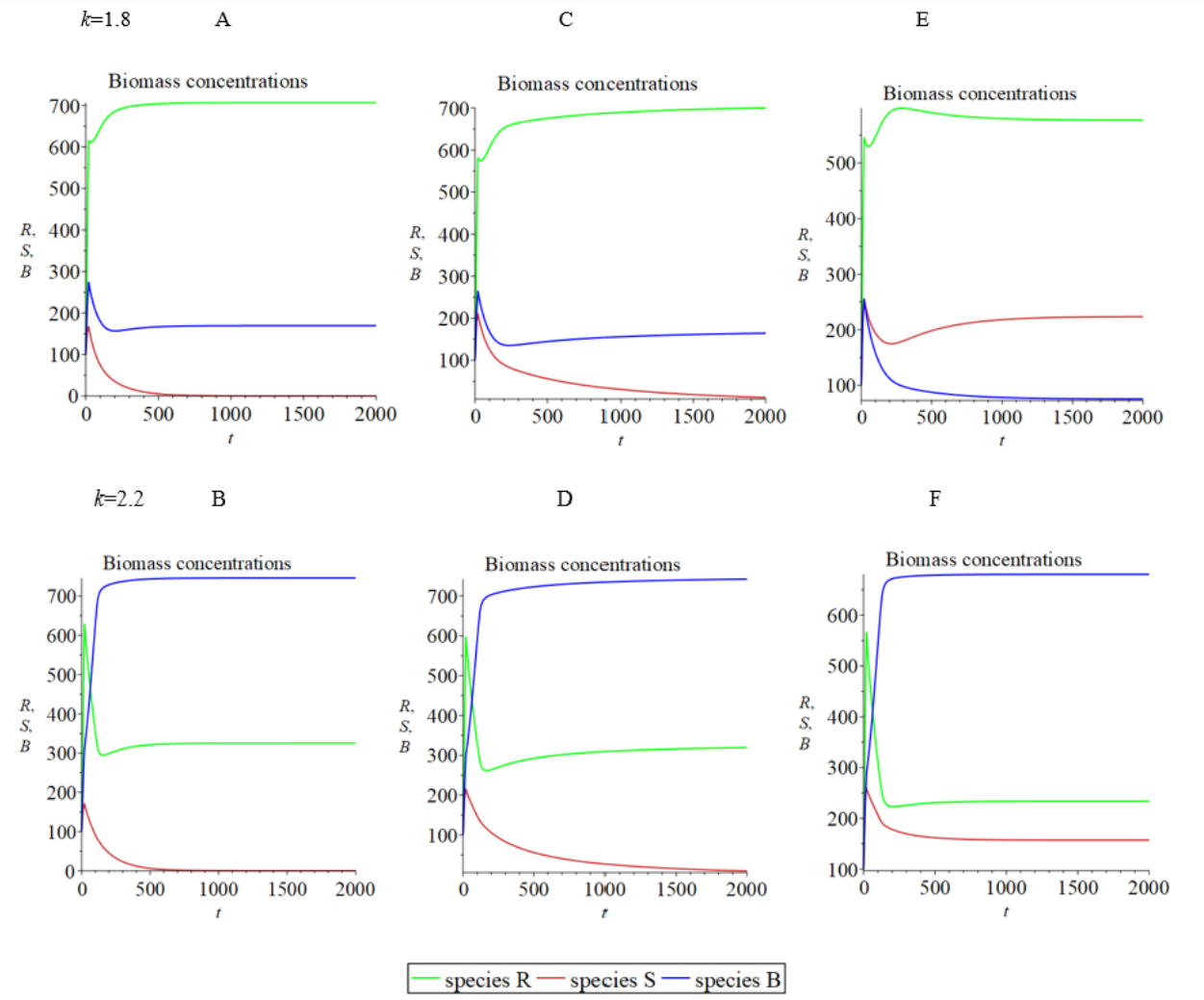


Figure 23: Simulations outcome for three species model. Parts A and B show results for $\mu_{\max,S} = 0.07$, parts C and D show results for $\mu_{\max,S} = 0.09$, parts E and F show results for $\mu_{\max,S} = 0.11$. Influent concentration of nitrate is 1000 μM.

Figure 23 illustrates the relationship between three species. Population S grows (as expected) with increasing $\mu_{\max,S}$, as it can be seen in parts A, C, E and B, D, F that show the simulation results for the same influent ratio but different growth rate values. We can see how the R and B domination is switched around between part A and B, C and D, and E and F. Each pair differs in the influent ratio, and again as it is expected, for smaller ratios, when carbon is limited (smaller k), R has a higher concentration, and when nitrate is limited (larger k), B has higher concentration.

However, the visible coexistence it is not necessarily a stable state, the biomass values are slowly changing

in time, so it is not clear if a stable three species coexistence is possible or it will slowly degrade to two species or one species only surviving. It is interesting to note that the coexistence stay for a really long time - most likely, it will continue well after $t = 2000$ when the simulation ends. It might mean that even if the species do not coexist stably, they might coexist long enough to make an impact to the environment.

As it was mentioned before, triple coexistence seems to enlarge the range of influent ratio k that make it possible to R and B survive together. For two species models, coexistence was stable for the range of $0.883 \leq k \leq 1.344$ while for three species systems, the coexistence lasts from roughly $k = 1.8$ up to $k = 2.4$ making it at least 30% wider than before. This might indicate an evolutionary benefit from multi-species communities for all participants.

4.3 Model's sensitivity analysis

In this section we will examine how sensitive the proposed model is to the newly introduced parameters' values, first of all those related to the third bacteria species, and to the affinity constants and yield values for nitrite for the denitrifiers and DNRA bacteria.

4.3.1 Latin Hypercube Sampling/Partial Rank Correlation Coefficient (LHS/PRCC) procedures

For the analysis, we will use Latin Hypercube Sampling/Partial Rank Correlation Coefficient (LHS/PRCC) procedures coupled with optimal control analysis described in [12]. The procedure combines Latin Hipercube sampling (LHS) and Partial Rank Correlation Coefficient (PRCC) analysis. During LHS, the range for parameters values is divided into equiprobable regions, and those regions are sampled once without replacement. For each range, a baseline value should be chosen. All the parameters should demonstrate monotonicity between a specific input and corresponding output variable. Simulations are run for each set of parameter values.

Then, all sampled values and the simulation outcomes are ranked from the smallest to the largest, and two linear regression models are found for each ranked parameter - one representing this ranked parameters in terms of the other ranked parameters, and the second model representing the corresponding ranked outcome measure in terms of the other ranked parameters values. Lastly, a correlation coefficient for the residual from those two regression provides the PRCC for this specific parameter. PRCC values lay between -1 and +1 and show how closely the change in the parameter correlates with the changes in the output variable in question. The correlation can be positive or negative, which is reflected in the PRCC value's

sign. Statistically significant results have a p-value smaller than 0.05.

For LHS/PRCC computation, we modified the MatLab code created as a part of [12] to make it suitable for the model (41) analysis.

4.3.2 LHS/PRCC model analysis

We want to find out the model's sensitivity to the growth rate, affinity constants, and yield values for the species S, and affinity constants and yields values for species R and B associated with nitrite reducing with biomass concentrations for bacterial species to be the output variables of the interest. We assume uniform distribution for the parameter range.

We included yields parameters into this list even though yield is not directly included in the equations fro biomass. However, the value of yield influences the substrate availability, and through that, the biomass concentration.

The interval of the parameters values as well as the baseline considered for the sensibility analysis are shown in the Table 11:

Table 11: Parameter values range and baseline values for PRCC analysis

parameter	meaning	units	range	baseline value
$\mu_{max,S}$	maximum growth rate for S	$\mu\mathrm{M\,h}^{-1}$	0.07..0.12	0.095
Y_{SN}	yield for unit of biomass of S per unit nitrate consumed	1	0.3..0.69	0.495
Y_{SC}	yield for unit of biomass of S per unit acetate consumed	1	0.39..0.586	0.488
Y_{RN2}	yield for unit of biomass of R per unit nitrite consumed	1	0.3..0.5	0.4
Y_{BN2}	yield for unit of biomass of B per unit nitrite consumed	1	0.55..0.65	0.6
K_{SN}	affinity constant for S to nitrate	μM	1.5..4.5	3
K_{SC}	affinity constant for S to acetate	μM	6..10	8
K_{RN2}	affinity constant for R to nitrite	μM	8..14	11
K_{BN2}	affinity constant for B to nitrite	μM	1..5	3

The choice of the range for parameter values was made based on the monotonicity between the specific input and the corresponding output variable, required for the procedure, and a more general context for the bacteria relationship in the model discussed in section 4.3. The baseline value is located at the centre of

the value range. The output variables are biomass concentrations of species R, B, and S. The analysis was performed for organic carbon to nitrate influent ratio $k = 1.8$ and $k = 2.2$ which both provide possibility for the tree species coexistence. The results of PRCC analysis are shown in Figure 24. All the PRCC values with a p-value > 0.05 (shown in gray) will be ignored as statistically insignificant. Statistically significant values are shown either in red ($PRCC > 0.5$ and $PRCC < -0.5$) or in blue ($PRCC < 0.5$ and $PRCC > -0.5$).

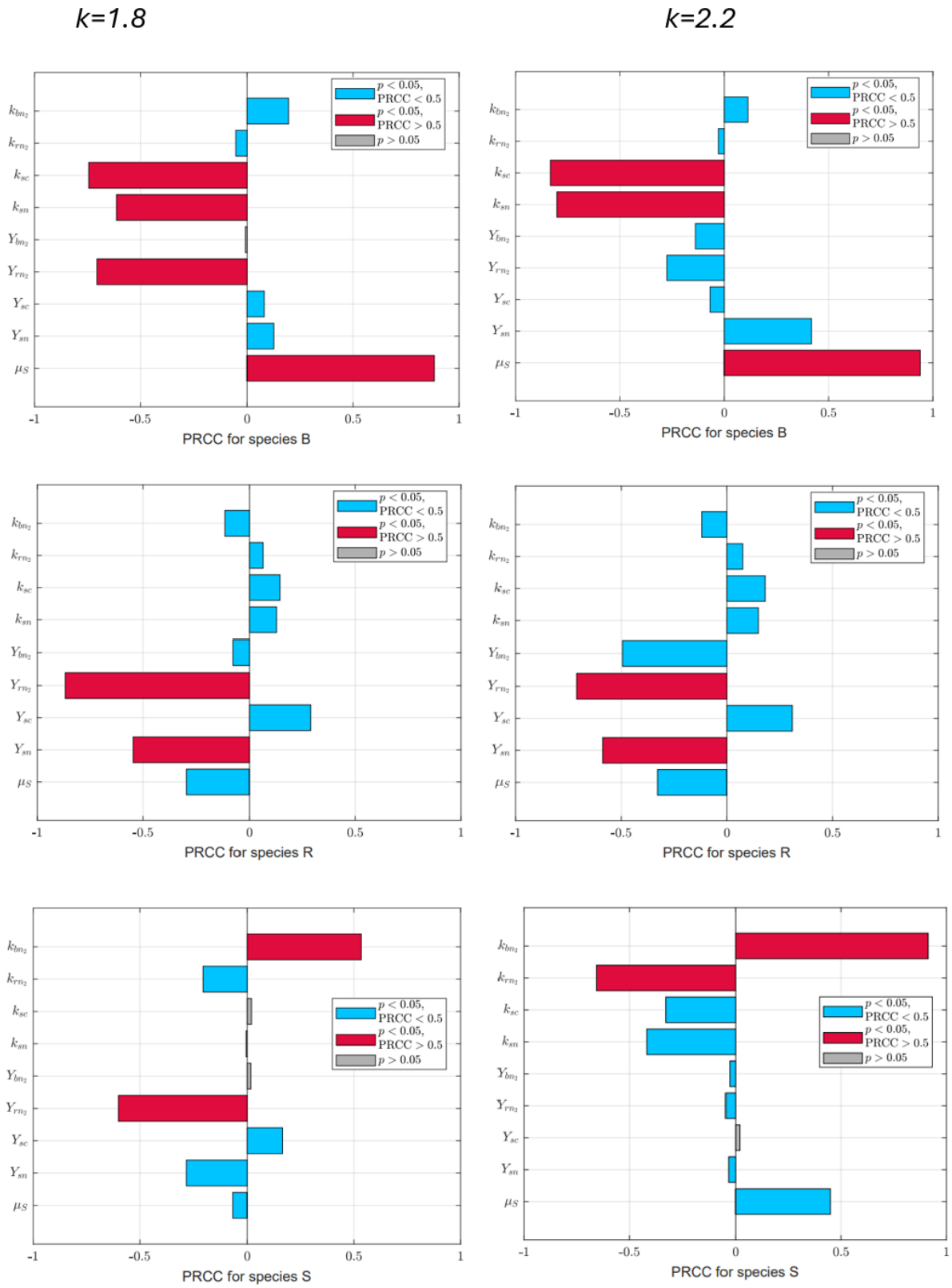


Figure 24: PRCC results for the model with C/N influent ratio k=1.8 and k=2.2. In both cases model predicts outcome with three bacterial species coexistence.

No parameters are shown contributing significantly to all three output variables but some results provide support to the hypothesized relationship between the bacteria in the three-species community. For example, we can see close connection between S and B in their relation to processing nitrate. The affinity constant for bacterium B on nitrite K_{BN2} is positively correlated with species S which can be interpreted as the increase in K_{BN2} value making B less efficient in processing nitrite so that is looses its advantage over S, and S has more resources to grow. On the other hand, the increase in affinity constant for S on nitrate K_{SN} has negative correlation with B biomass, since less efficient S produces less NO_2 for other bacteria to use. The maximum growth rate of S μ_S has positive correlation with B and negative with R, which might reflect the fact that due to close value of affinity constants S and B react similarly to the changing environmental conditions. However, growth of S takes resources from R and has a negative impact on its biomass growth.

However, the PRCC analysis does not suggest any straightforward way to produce a simplified three species system as there are no parameters that are found not contributing significantly to the values of all three output variables.

4.4 Summary

We have built a three species system that represents denitrification and DNRA as two step reactions and includes three bacterial species. A set of parameters values was used for simulations that demonstrate the possibility of triple and double coexistence equilibiria in such a system. However, the increased complexity of the model makes its analysis very problematic.

5 Chapter 5: Conclusion and future work

Nitrogen in soil goes through various bacteria enabled processes that participate in the global nitrogen cycle. Two of those processes - denitrification and dissimilatory nitrate reduction to ammonium (DNRA) - happen under similar conditions (low oxygen levels) but lead to different consequences for the environment: denitrification results in gaseous nitrogen containing compounds released to the atmosphere while DNRA leads to ammonium accumulation in the soils. Mathematical modelling of denitritfication and DNRA reactions can help in better understanding the conditions for both reactions and estimating the consequences of soil fertilization for the environment.

The first model analysed in Chapter 2 describes two bacterial species competition (denitrifiers and DNRA performing bacteria) over two substrates - nitrate and organic carbon. The bacterial growth rate definition includes Liebig's minimum principle so that only the most limited substrate influences the biomass growth. We have found 5 steady states for the model and the feasibility conditions for each. However, due to a non-differentiable function in the model formulation, we could only rely on simulations to investigate the steady states stability. Overall, we have found the final states solutions for all five steady states and deduced the stability conditions for them.

In Chaper 3, we created a more realistic model by modifying the bacterial growth rate definition to include two Monod terms, one for each substrate. We found the steady states for the second model and performed stability analysis using standard methods. As a result, we were able to make a more general picture of the systems modelling two bacterial species competition. We have shown the correlation between system parameters and the steady states stability. In particular, we have found the settings requirements for four possible system configurations that would lead to different outcomes - two configurations that would lead to one species domination and two configurations that can result in a stable two species coexistence.

Comparison between systems (9) and (12) predictions and experimental data shows that both models perform well for a system in saturation.

It might be interesting to compare the models' predictions for a system under starvation conditions, if experimental data becomes available. A theoretical analysis of the model (12) assuming starvation conditions would require different non-dimensionalizing steps and parameters grouping and new stability analysis approach. However, understanding the mechanism of denitirfiers and DNRA performing bacteria competition under all spectrum of conditions, from starvation to saturation, might be useful for application to different types of soil.

In both Chapter 2 and Chpater 3, we considered denitrification and DNRA as one step reactions

performed by a single bacterial species. However, there is much evidence that many bacteria are able to perform only some but not all steps of nitrogen reduction [25], [33],[21], and a complete denitrification or DNRA might depend on multiple species cooperation. In chapter 4, we introduce a model (41) for truncated denitrification with three bacterial species included. In the model, three bacterial species compete for nitrate, and two species only compete for nitrite. Numerical simulations with chosen parameter values show that triple coexistence is possible, and it actually provides a widened range of influent concentrations ratio for denitrifiers and DNRA able bacteria coexistence. This result aligns well with the experimental evidence that a multiple bacterial species community might be beneficial for its participants ([4], [41]).

Due to system (41) complexity, we could not perform steady state analysis in a straightforward way. Furthermore, there was no obvious model reduction strategies as the sensitivity analysis showed that there were no parameters that were non significant for all three species' growth.

For future study, further investigation needs to be done in the possible ways of non-dimensionalization for model (41) that would facilitate the system's analysis. Another direction would be to create a reduced system for fixed set of parameters that would lead to a specific outcome of an interest (e.g. triple coexistence) and perform an analysis on it. When more experimental data is available for truncated denitrification and DNRA and the corresponding bacterial species, we can hope to reduce the model's uncertainty by reconsidering the parameter choices and the implications for the system's possible outcomes.

Another important note is that all models considered in this project were built under assumption that influent concentration is constant for the time of the experiment/simulation. However, it might not be true for the real-life situation when nitrogen or carbon influx might change with time. Those fluctuation will necessarily change species' dynamics. For future work, it might be interesting to see how the model can be adjusted for a fluctuating influent ratio defined as a function of time $k = f(t)$ and look into its steady states.

6 List of acronyms

1. anammox - Anaerobic Ammonium Oxidation
2. COD - Chemical Oxygen Demand
3. DNRA - Dissimilatory Nitrate Reduction to Ammonium
4. IC - Initial Conditions
5. LHS - Latin Hypercube Sampling
6. PCR - Polymerase Chain Reaction
7. PRCC - Partial Rank Correlation Coefficient

7 Bibliography

References

[1] Abbamondi, G. R., Tommonaro, G., Weyens, N., Thijs, S., Sillen, W., Gkorezis, P., Iodice, C., de Melo Rangel, W., Nicolaus, B., Vangronsveld, J. (2016). Plant growth-promoting effects of rhizospheric and endophytic bacteria associated with different tomato cultivars and new tomato hybrids. Chemical and Biological Technologies in Agriculture, 3(1). https://doi.org/10.1186/s40538-015-0051-3

[2] Canada, A. and A.-F. (2021, June 3). Government of Canada. Agriculture and Agri-Food Canada. https://agriculture.canada.ca/en/agricultural-production/water/nitrogen-indicator

[3] Chakrawal, A., Calabrese, S., Herrmann, A. M., Manzoni, S. (2022). Interacting bioenergetic and stoichiometric controls on Microbial Growth. Frontiers in Microbiology, 13. https://doi.org/10.3389/fmicb.2022.859063

[4] Chang, C.-Y., Bajić, D., Vila, J. C., Estrela, S., Sanchez, A. (2023). Emergent coexistence in multispecies microbial communities. Science, 381(6655), 343–348. https://doi.org/10.1126/science.adg0727

[5] Del Grosso, S. J., Smith, W., Kraus, D., Massad, R. S., Vogeler, I., Fuchs, K. (2020). Approaches and concepts of modelling denitrification: Increased process understanding using observational data can reduce uncertainties. Current Opinion in Environmental Sustainability, 47, 37–45. https://doi.org/10.1016/j.cosust.2020.07.003

[6] De Mazancourt, C., Schwartz, M. W. (2010). A resource ratio theory of cooperation. Ecology Letters, 13(3), 349–359. https://doi.org/10.1111/j.1461-0248.2009.01431.x

[7] Dlamini, J. C., Chadwick, D., Hawkins, J. M., Martinez, J., Scholefield, D., Ma, Y., Cárdenas, L. M. (2020). Evaluating the potential of different carbon sources to promote denitrification. The Journal of Agricultural Science, 158(3), 194–205. https://doi.org/10.1017/s0021859620000520

[8] Dodla, S., Wang, J., Delaune, R., Cook, R. (2008). Denitrification potential and its relation to organic carbon quality in three coastal wetland soils. Science of The Total Environment, 407(1), 471–480. https://doi.org/10.1016/j.scitotenv.2008.08.022

[9] Galloway, J. N., Leach, A. M., Bleeker, A., Erisman, J. W. (2013). A chronology of human understanding of the nitrogen cycle. Philosophical Transactions of the Royal Society B: Biological Sciences, 368(1621), 20130120. https://doi.org/10.1098/rstb.2013.0120

[10] Gamble, T. N., Betlach, M. R., Tiedje, J. M. (1977). Numerically dominant denitrifying bacteria from world soils. Applied and Environmental Microbiology, 33(4), 926–939. https://doi.org/10.1128/aem.33.4.926-939.1977

[11] Giles, M., Morley, N., Baggs, E. M., Daniell, T. J. (2012). Soil nitrate reducing processes – drivers, mechanisms for spatial variation, and significance for nitrous oxide production. Frontiers in Microbiology, 3. https://doi.org/10.3389/fmicb.2012.00407

[12] Gomero, B. (2012). Latin hypercube sampling and partial rank correlation coefficient analysis applied to an optimal control problem (dissertation). Latin Hypercube Sampling and Partial Rank Correlation Coefficient analysis applied to an optimal control problem.

[13] Groffman, P., Butterbach-Bahl, K., Fulweiler, R., Gold, A., Morse, J., Stander, E., et al. (2009). Challenges to incorporating spatially and temporally explicit phenomena (hotspots and hot moments) in denitrification models. Biogeochemistry 93, 49–77. doi: 10.1007/s10533-008-9277-5

[14] Gujer, W., Henze, M., Mino, T., van Loosdrecht, M. (1999). Activated sludge model no. 3. Water Science and Technology, 39(1), 183–193. https://doi.org/10.2166/wst.1999.0039

[15] Guo, L., Yu, H., Niu, W., Kharbach, M. (2021). Biochar promotes nitrogen transformation and tomato yield by regulating nitrogen-related microorganisms in tomato cultivation soil. Agronomy, 11(2), 381. https://doi.org/10.3390/agronomy11020381

[16] Hardison, A. K., Algar, C. K., Giblin, A. E., Rich, J. J. (2015). Influence of organic carbon and nitrate loading on partitioning between dissimilatory nitrate reduction to ammonium (DNRA) and N2 production. Geochimica et Cosmochimica Acta, 164, 146–160. https://doi.org/10.1016/j.gca.2015.04.049

[17] Heinen, M. (2006). Simplified denitrification models: Overview and properties. Geoderma, 133(3–4), 444–463. https://doi.org/10.1016/j.geoderma.2005.06.010

[18] Ishizawa, H., Tashiro, Y., Inoue, D., Ike, M., Futamata, H. (2024). Learning beyond-pairwise interactions enables the bottom–up prediction of Microbial Community Structure. Proceedings of the National Academy of Sciences, 121(7). https://doi.org/10.1073/pnas.2312396121

[19] Jabot, F., Pottier, J. (2012). A general modelling framework for resource-ratio and csr theories of plant community dynamics. Journal of Ecology, 100(6), 1296–1302. https://doi.org/10.1111/j.1365-2745.2012.02024.x

[20] Jia, M., Winkler, M. K., Volcke, E. I. (2020). Elucidating the competition between heterotrophic denitrification and DNRA using the resource-ratio theory. Environmental Science; Technology, 54(21), 13953–13962. https://doi.org/10.1021/acs.est.0c01776

[21] Kandeler, E., Brune, T., Enowashu, E., Dörr, N., Guggenberger, G., Lamersdorf, N., Philippot, L. (2009). Response of total and nitrate-dissimilating bacteria to reduced n deposition in a spruce forest soil profile. FEMS Microbiology Ecology, 67(3), 444–454. https://doi.org/10.1111/j.1574-6941.2008.00632.x

[22] Koop-Jakobsen, K., Giblin, A. E. (2010). The effect of increased nitrate loading on nitrate reduction via denitrification and DNRA in salt marsh sediments. Limnology and Oceanography, 55(2), 789–802. https://doi.org/10.4319/lo.2010.55.2.0789

[23] Kraft, B., Strous, M., Tegetmeyer, H. E. (2011). Microbial nitrate respiration – genes, enzymes and environmental distribution. Journal of Biotechnology, 155(1), 104–117. https://doi.org/10.1016/j.jbiotec.2010.12.025

[24] Langergraber, G., Rousseau, D. P., García, J., Mena, J. (2009). CWM1: A general model to describe biokinetic processes in subsurface flow constructed wetlands. Water Science and Technology, 59(9), 1687–1697. https://doi.org/10.2166/wst.2009.131

[25] Lycus, P., Lovise Bøthun, K., Bergaust, L., Peele Shapleigh, J., Reier Bakken, L., Frostegård, Å. (2017). Phenotypic and genotypic richness of denitrifiers revealed by a novel isolation strategy. The ISME Journal, 11(10), 2219–2232. https://doi.org/10.1038/ismej.2017.82

[26] MacArthur, R. H. (1972). Geographical ecology: Patterns in the distribution of species. Harper and Row.

[27] Moreno-Vivian, C., Cabello, P., Martinez-Luque, M., Blasco, R., Castillo, F. (1999). Prokaryotic nitrate reduction: Molecular properties and functional distinction among bacterial nitrate reductases. Journal of Bacteriology, 181(21), 6573-6584. https://doi.org/10.1128/jb.181.21.6573-6584.1999

[28] Miller, Burns, Munguia, Walters, Kneitel, Richards, Mouquet, Buckley. (2005). A critical review of twenty years' use of the resource-ratio theory. The American Naturalist, 165(4), 439. https://doi.org/10.2307/3473474

[29] Moyles, I. R., Fowler, A. C. (2018). Production of nitrate spikes in a model of ammonium biodegradation. Theoretical Ecology, 11(3), 333–350. https://doi.org/10.1007/s12080-018-0370-7

[30] Pepper, I. L., Gerba, C. P., Gentry, T. J. (2015). Environmental microbiology. Elsevier.

[31] Pan, S.-Y., He, K.-H., Lin, K.-T., Fan, C., Chang, C.-T. (2022). Addressing nitrogenous gases from croplands toward low-emission agriculture. Npj Climate and Atmospheric Science, 5(1). https://doi.org/10.1038/s41612-022-00265-3

[32] Qasim, W., Zhao, Y., Wan, L., Lv, H., Lin, S., Gettel, G. M., Butterbach-Bahl, K. (2021). The potential importance of soil denitrification as a major N loss pathway in intensive greenhouse vegetable production systems. Plant and Soil, 471(1–2), 157–174. https://doi.org/10.1007/s11104-021-05187-2

[33] Rütting, T., Boeckx, P., Müller, C., Klemedtsson, L. (2011a). Assessment of the importance of dissimilatory nitrate reduction to ammonium for the terrestrial nitrogen cycle. Biogeosciences, 8(7), 1779–1791. https://doi.org/10.5194/bg-8-1779-2011

[34] Sundarraman, D., Hay, E. A., Martins, D. M., Shields, D. S., Pettinari, N. L., Parthasarathy, R. (2020). Higher-order interactions dampen pairwise competition in the zebrafish gut microbiome. mBio, 11(5). https://doi.org/10.1128/mbio.01667-20

[35] Scheer, C., Fuchs, K., Pelster, D. E., Butterbach-Bahl, K. (2020). Estimating global terrestrial denitrification from measured N2o:(N2o+N2) product ratios. Current Opinion in Environmental Sustainability, 47, 72–80. https://doi.org/10.1016/j.cosust.2020.07.005

[36] Schlüter, S., Henjes, S., Zawallich, J., Bergaust, L., Horn, M., Ippisch, O., Vogel, H.-J., Dörsch, P. (2018). Denitrification in soil aggregate analogues-effect of aggregate size and oxygen diffusion. Frontiers in Environmental Science, 6. https://doi.org/10.3389/fenvs.2018.00017

[37] Shapleigh J. (2013). Denitrifying Prokaryotes. In:Rosenbers E (ed). The Prokaryotes, Fourth edn. Springer-Verlag, Berlin, Heidelberg, pp 405–425

[38] Sharma, S., Aneja, M. K., Mayer, J., Munch, J. C., Schloter, M. (2005). Diversity of transcripts of nitrite reductase genes (nirk and nirs) in rhizospheres of grain legumes. Applied and Environmental Microbiology, 71(4), 2001–2007. https://doi.org/10.1128/aem.71.4.2001-2007.2005

[39] Silver, W. L., Herman, D. J., Firestone, M. K. (2001). Dissimilatory nitrate reduction to ammonium in upland tropical forest soils. Ecology, 82(9), 2410–2416. https://doi.org/10.1890/0012-9658(2001)082[2410:dnrtai]2.0.co;2

[40] Sparacino-Watkins, C., Stolz, J. F., Basu, P. (2014). Nitrate and periplasmic nitrate reductases. Chem. Soc. Rev., 43(2), 676–706. https://doi.org/10.1039/c3cs60249d

[41] Stubbendieck, R. M., Vargas-Bautista, C., Straight, P. D. (2016). Bacterial communities: Interactions to scale. Frontiers in Microbiology, 7. https://doi.org/10.3389/fmicb.2016.01234

[42] Surey, R., Schimpf, C. M., Sauheitl, L., Mueller, C. W., Rummel, P. S., Dittert, K., Kaiser, K., Böttcher, J., Mikutta, R. (2020). Potential denitrification stimulated by water-soluble organic carbon from plant residues during initial decomposition. Soil Biology and Biochemistry, 147, 107841. https://doi.org/10.1016/j.soilbio.2020.107841

[43] Tang, J., Riley, W. J. (2021). Finding liebig's law of the minimum. Ecological Applications, 31(8). https://doi.org/10.1002/eap.2458

[44] Tiedje, J. M. Ecology of Denitrification and Dissimilatory Nitrate Reduction to Ammonium. In Biology of Anaerobic Microorganisms; Zehnder, A. J. B., Ed.; John Wiley and Sons: New York, 1998; pp 179-244

[45] Tiedje, J. M., Sexstone, A. J., Myrold, D. D., Robinson, J. A. (1983). Denitrification: Ecological niches, competition and survival. Antonie van Leeuwenhoek, 48(6), 569–583. https://doi.org/10.1007/bf00399542

[46] Tilman, D. (1982). Resource Competition and Community Structure. Princeton University Press.

[47] Tobias, C. R., Macko, S. A., Anderson, I. C., Canuel, E. A., Harvey, J. W. (2001). Tracking the fate of a high concentration groundwater nitrate plume through a fringing marsh: A combined groundwater tracer and in situ isotope enrichment study. Limnology and Oceanography, 46(8), 1977–1989. https://doi.org/10.4319/lo.2001.46.8.1977

[48] van den Berg, E. M., Boleij, M., Kuenen, J. G., Kleerebezem, R., van Loosdrecht, M. C. (2016). DNRA and denitrification coexist over a broad range of acetate/N-NO3 - ratios, in a chemostat enrichment culture. Frontiers in Microbiology, 7. https://doi.org/10.3389/fmicb.2016.01842

[49] van den Berg, E. M., van Dongen, U., Abbas, B., van Loosdrecht, M. C. (2015). Enrichment of DNRA bacteria in a continuous culture. The ISME Journal, 9(10), 2153–2161. https://doi.org/10.1038/ismej.2015.26

[50] van den Berg, E. M., Elisário, M. P., Kuenen, J. G., Kleerebezem, R., van Loosdrecht, M. C. (2017). Fermentative bacteria influence the competition between denitrifiers and DNRA bacteria. Frontiers in Microbiology, 8. https://doi.org/10.3389/fmicb.2017.01684

[51] Wei, W., Isobe, K., Nishizawa, T., Zhu, L., Shiratori, Y., Ohte, N., Koba, K., Otsuka, S., Senoo, K. (2015). Higher diversity and abundance of denitrifying microorganisms in environments than considered previously. The ISME Journal, 9(9), 1954–1965. https://doi.org/10.1038/ismej.2015.9

[52] Yang, Y., Liu, H., Lv, J. (2022). Response of N2O emission and denitrification genes to different inorganic and organic amendments. Scientific Reports, 12(1). https://doi.org/10.1038/s41598-022-07753-9

[53] Zhang, X., Tong, S., Jia, C., Zhang, W., Wang, Z., Tang, G., Hu, B., Liu, Z., Wang, L., Zhao, P., Pan, Y., Ge, M. (2023). Elucidating hono formation mechanism and its essential contribution to oh during haze events. Npj Climate and Atmospheric Science, 6(1). https://doi.org/10.1038/s41612-023-00371-w